Charles University in Prague
Faculty of Science

Study Programme: Biology

Branch of Study: Genetics, Molecular Biology and Virology

Curriculum: Molecular Biology and Genetics of Eucaryotes

Bc. Radmila Hanečková

Generation and Analysis of Double-deficient Transgenic Mice for Kallikrein-related Peptidase 5 and Kallikrein-related Peptidase 14

Tvorba a Analýza Dvojnásobně Deficientních Trasgenních Myší pro Kalikrein 5 a Kalikrein 14

Master Thesis

Supervisor: RNDr. Radislav Sedláček, Ph.D.

Consultant: Mgr. Petr Kašpárek

Laboratory of Transgenic Models of Diseases

Institute of Molecular Genetics of the ASCR

Prague, 2016

Prohlášení:

Prohlašuji, že jsem závěrečnou práci zpracovala samostatně a že jsem uvedla všechny použité informační zdroje a literaturu. Tato práce ani její podstatná část nebyla předložena k získání jiného nebo stejného akademického titulu.

V Praze, 9. 8. 2016

I would like to thank my supervisor Radislav Sedláček for giving me a generous opportunity to pursue such challenging research and to my consultant Petr Kašpárek for guiding me through it with patience and advice whenever I needed it. I would also like to acknowledge the significant contribution to this research by the technicians of the Czech Center of Phenogenomics.

Finally, I am greatly indebted to my husband, Petr Baudiš, as well as to my family and friends for giving me untiring support without hesitation, despite my sudden decision to give up my artistic career to become a molecular geneticist at age 25.

Abstract

Kallikrein-related peptidases (KLKs) constitute a highly conserved serine protease family. Based on *in vitro* experiments, KLKs are predicted to play an important role in a number of physiological and pathophysiological processes. However, their role *in vivo* remains not fully understood, partially due to a lack of suitable animal models. In this work, we aim to prepare a KLK5 and KLK14 double-deficient mouse model. Both KLK5 and KLK14 were proposed to be involved in epidermal proteolytic networks critical for maintaining skin homeostasis. However, both KLK5 and KLK14 single-deficient mouse models show minimal or no phenotype, likely due to similar substrate specificity resulting in functional compensation. Double-deficient mice cannot be easily obtained by crossing due to localization of the *Klk5* and *Klk14* genes within the same locus on chromosome 7. We report that KLK5 and KLK14 double-deficient mice were successfully generated, mediated by transcription activator-like effector nucleases (TALENs) targeting *Klk14* by microinjection of TALEN mRNA into KLK5-deficient zygotes. Furthermore, we show that KLK5 and KLK14 double-deficient mice are viable and fertile. We believe that these novel mouse models may serve as a useful experimental tool to study KLK5 and KLK14 *in vivo*.

Keywords

KLK14, KLK5, epidermis, skin homeostasis, Netherton syndrome, transgenic technologies, TALEN, CRISPR/Cas9, programmable nucleases, mouse model

Abstrakt

Peptidázy příbuzné kalikreinu (KLK) představují vysoce konzervovanou rodinu serinových proteáz. *In vitro* experimenty naznačují, že KLK peptidázy hrají důležitou roli v řadě fyziologických a patofyziologických procesů. Jejich úloha *in vivo* ovšem zůstává ne zcela probádaná, částečně i kvůli nedostatku vhodných zvířecích modelů. Cílem této práce je příprava myšího modelu dvojnásobně deficientního na KLK5 a KLK14. Předpokládá se, že KLK5 a KLK14 jsou součástí proteolytických sítí v pokožce, které jsou významné pro udržení homeostáze kůže. Ovšem myší modely deficientní pouze na KLK5 nebo KLK14 vykazují jenom minimální či žádný fenotyp, pravděpodobně kvůli vzájemné funkční kompenzaci na základě podobné substrátové specifity. V této práci popisujeme úspěšné vytvoření myši dvojnásobně deficientní na KLK5 a KLK14. Dvojnásobně deficientní myši nelze snadno získat křížením kvůli přítomnosti genů pro *Klk5* a *Klk14* ve stejném lokusu na chromozomu 7, proto k tvorbě myšího modelu používáme TAL efektor nukleázy (TALENy) cílené na *Klk14*, které aplikujeme mikroinjekcí TALENové mRNA do KLK5-deficientních zygot. Dále ukazujeme, že myši dvojnásobně deficientní na KLK5 a KLK14 jsou životaschopné a plodné. Domníváme se, že tyto nové myší modely mohou sloužit jako užitečný experimentální nástroj ke studiu KLK5 a KLK14 *in vivo*.

Klíčová slova

KLK14, KLK5, epidermis, homeostáze kůže, Nethertonův syndrom, transgenní technologie, TALEN, CRISPR/Cas9, programovatelné nukleázy, myší model

Table of Contents

1. List of Abbreviations

AD	Atopic dermatitis
Cas9	CRISPR associated protein 9
CRISPR	Clustered regularly interspaced short palindromic repeats
DMEM	Dulbecco's Modified Eagle Medium
DSB	Double strand break
ESC	Embryonic stem cell
GFP	Green fluorescence protein
gRNA	Guide RNA
hCG	Human chorionic gonadotropin hormone
IL8	Interleukin 8
IPTG	Isopropyl beta-D-1-thiogalactopyranoside
KLK	Kallikrein-related peptidase
KO	Knock-out
LB	Luria broth
LEKTI	Lympho-epithelial Kazal-type related inhibitor
MCS	Multiple cloning site
MMEJ	Microhomology-mediated end-joining
M-MLV	Moloney murine leukemia virus
NHEJ	Non-homologous end-joining
NS	Netherton syndrome
P	Postnatal day
PAM	Protospacer adjacent motif
PAR2	Proteinase-activated receptor 2
PBS	Phosphate buffered saline
PCR	Polymerase chain reaction
PN	Programmable nuclease
RFLP	Restriction fragment length polymorphism
RFP	Red fluorescence protein
RVD	Repeat-variable di-residue
SPINK5	Serine protease inhibitor Kazal-type 5
TALEN	Transcription activator-like effector nuclease
TSLP	Thymic stromal lymphopoietin
WT	Wild type

2. Introduction

The laboratory mouse (*Mus musculus*) as a model organism has a long history. Its relatively short reproductive cycle, large litter size, and most importantly, its close similarity to human physiology and underlying genome structure render it an ideal candidate for the exploration of molecular mechanisms governing human disease (ZHENG-BRADLEY *et al.* 2010). To this effect, large-scale international initiatives have been launched that endeavor to prepare knock-out mouse strains, targeting all identified murine genes (BROWN *et al.* 2012, RYDER *et al.* 2013). Our laboratory is part of the Czech Centre for Phenogenomics and participates in the global effort of characterizing the already available mouse strains, as well as generating novel models. Recently, due to the advent of genome editing using programmable nucleases (PNs), new possibilities of preparing knock-out and transgenic mouse models have emerged. In addition to the traditional embryonic stem cell (ESC) approach, microinjection of PNs directly into zygotes is being widely employed as an alternative (WEFERS *et al.* 2013, FUJII *et al.* 2013). At our laboratory, we have already established the generation of transgenic mice using transcription activator-like effector nuclease (TALEN) technology (KASPAREK *et al.* 2014). Additionally, we have developed a surrogate reporter system that can be used in conjunction with both TALENs and the more recent PN technology, the clustered regularly interspaced short palindromic repeats (CRISPR)/Cas9 toolkit. The surrogate reporter system enables us to verify PN activity in cell culture, enrich for positively targeted cells and screen for putative off-target sites (KASPAREK *et al.* 2014, HANECKOVA 2016).

Already, there are over a thousand human diseases that have their corresponding mouse model. The preparation and phenotyping of these mouse models is expected to provide insight into gene function in the context of the complexity of a mammalian organism and lead to the development of effective treatment of human disease. At the center of our current efforts is the analysis of physiologically and pathophysiologically important KLK proteolytic networks. An example of pathophysiology due to KLK dysregulation is Netherton syndrome (NS), a severe congenital ichthyosiform disease caused by mutations in an epidermal serine protease inhibitor, LEKTI (lympho-epithelial Kazal-type related inhibitor). In the absence of LEKTI, increased shedding of corneocytes, epithelial dehydration and persistent inflammation are NS symptoms that have been linked to serine proteases of the kallikrein-related peptidase (KLK) family, but their interplay and individual roles in the epidermis remain to be fully explored (FURIO *et al.* 2015). For this purpose, we are working on the preparation and phenotyping of several KLK-deficient mouse strains that we hope will broaden our understanding of the complex proteolytic cascades involved in maintaining epidermal homeostasis. Though NS is a relatively rare condition, other skin diseases such as atopic dermatitis (AD) are much more prevalent. The prevalence of AD in particular has been increasing in recent years, especially in urban areas (MORTZ *et al.* 2015). Interestingly, AD has been linked to epidermal barrier dysfunction due to genetic predisposition (ELIAS *et al.* 2009). Our KLK-deficient mouse models therefore could provide a tool to explore the molecular mechanisms underlying a variety of human epidermal diseases, not just Netherton syndrome.

3. Aims of the Thesis

The main aim of this work is to generate a novel mouse strain, double-deficient for both kallikrein-related peptidase 5 (KLK5) and kallikrein-related peptidase 14 (KLK14). The proposed strategy is microinjection of programmable nuclease (PN) mRNA targeting *Klk14* into $Klk5^{tm2a(KOMP)Wtsi}$ ($Klk5^{-/-}$) zygotes. This involves the following:

- Selection of suitable target loci within the *Klk14* gene
- Design of transcription activator-like effector nucleases (TALENs) and guide RNA (gRNA) for cloning into a CRISPR/Cas9 expression vector
- Preparation of vectors expressing the PNs employing molecular cloning techniques
- Verification of PN cleavage activity
- Preparation of PN mRNA for microinjection
- Characterization, genotyping and selection of suitable founder mice for establishing a KLK5 and KLK14 double-deficient mouse strain
- Breeding for the production of knock-out individuals
- Preliminary characterization of KLK5 and KLK14 double-deficient phenotype with main focus on the epidermis

4. Literature Review

4.1. The Kallikrein-related Peptidase (KLK) Family of Serine Proteases

The human kallikrein-related peptidase (KLK) family constitutes 15 trypsin- and chymotrypsin-like serine proteases (PAVLOPOPULOU *et al.* 2010). Expressed as single chain preproenzymes, KLKs are proteolytically processed to inactive proenzymes and secreted into the extracellular space where they are activated by proteolytic cleavage. Members of the KLK family are highly conserved proteases of around 250 amino acids in length, display at least 40 % protein identity, and have a common catalytic triad consisting of His, Ser and Gly amino acid residues responsible for stabilizing the substrate during hydrolysis in their active site (Fig. 1).

Figure 1. Catalytic motifs present in all members of the KLK family. The height of each letter corresponds to the frequency with which each residue occurs in the KLK catalytic site. The His, Asp and Ser catalytic triad (asterisks) is highly conserved between individual KLKs across different species (adapted from PAVLOPOPULOU *et al.* 2010).

In the human genome, all 15 members of the KLK family are encoded by a large contiguous gene cluster on chromosome 19 with all of the transcripts having virtually identical splicing patterns consisting of 5 exons for each KLK gene. Both the structure of the KLK gene locus and the KLK family proteases display high evolutionary conservation between mammalian genomes (LUNDWALL 2013). Consequently, this is the case for the human and the laboratory mouse (*Mus musculus*) KLK gene family (OLSSON *et al.* 2002, PAVLOPOPULOU *et al.* 2010). In the mouse, the KLK gene cluster is localized on chromosome 7 (Fig. 2).

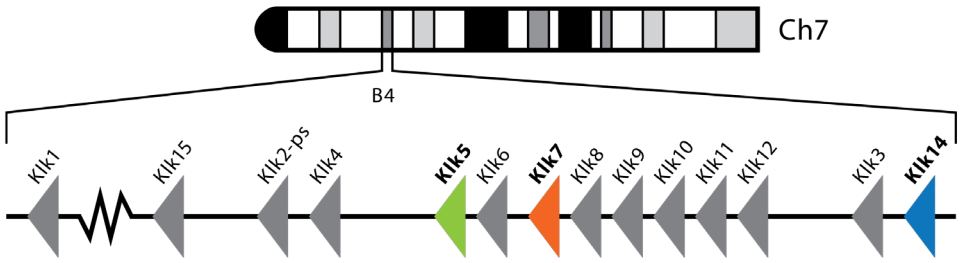

Figure 2. The Mus musculus KLK gene locus. The genes encoding murine KLKs all cluster in B4 on chromosome 7.

The KLK protease family shows ubiquitous expression across a variety of tissues. Individual members of the family are implicated to play a role in key physiological processes such as seminal plasma liquefaction, tooth development and skin homeostasis (BRATTSAND *et al.* 2005, EMAMI *et al.* 2008, SMITH *et al.* 2011). Additionally, several KLKs are known tumour markers and changes in their expression have been linked to cancer development and prognosis (TALIERI *et al.* 2012, DRUCKER *et al.* 2015).

4.2. The Role of Kallikrein-related Peptidases in Skin Homeostasis and Netherton Syndrome

The mammalian skin is a complex organ, characterized by a stratified epithelium organisation that is closely linked to its protective barrier function – the epidermal layer provides protection against UV radiation, water loss, and various other environmental challenges including bacterial infections. Constant renewal of epidermal cells is central to epidermal barrier integrity. Keratinocytes are continuously produced by proliferation of basal layer stem cells within the deepest epidermal layer, the *stratum basale* (CANDI *et al.* 2005). The keratinocytes differentiate while progressing upwards through the *stratum spinosum* and *stratum granulosum*. During differentiation, keratinocytes eventually lose nuclei and organelles and transform into corneocytes that form the *stratum corneum*, the topmost epidermal layer (Fig. 3). The differentiating epidermal layers are also characterized by the presence of pH and Ca^{2+} gradients. pH becomes acidic in the topmost *stratum corneum* layer, and Ca^{2+} concentration continually rises until the *stratum granulosum* and

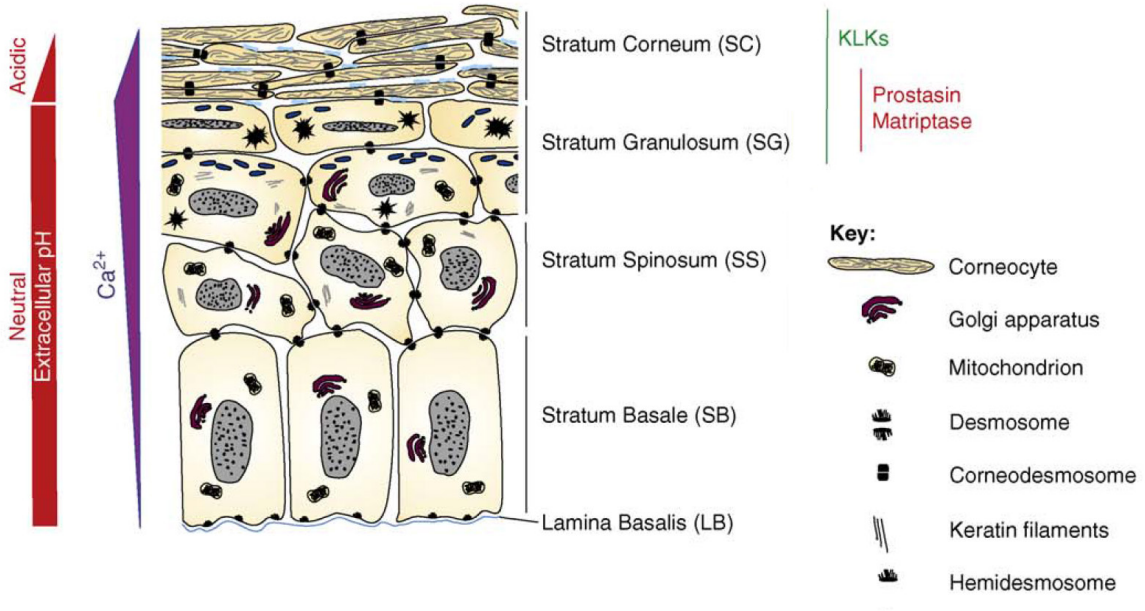

Figure 3. Organization of the stratified epidermal epithelium. Keratinocytes continually proliferate in the *stratum basale*, travel upwards and differentiate into corneocytes in the *stratum granulosum*, accumulating a dense keratin network while losing nuclei and organelles. In the top-most *stratum corneum* layer (characterized by acidic pH and decrease of Ca^{2+} concentration), corneodesmosomes derived from desmosomes are proteolytically cleaved and individual corneocytes are shed continually in a process termed desquamation (Adapted from OVAERE *et al.* 2009).

decreases again in the *stratum corneum* (MENON *et al.* 1992, OHMAN et al. 1994). Corneocytes contain a dense keratin network and adhere to each other via corneodesmosomes – structures derived from desmosomes made up of several corneodesmosomal proteins, notably corneodesmosin, desmoglein 1 and desmocollin 1 (CAUBET *et al.* 2004). Corneocytes are continually shed from the *stratum corneum* in a process termed desquamation, an important process essential for renewal of the epidermis and maintenance of its barrier function (CANDI *et al.* 2005).

4.2.1. Proteolytic Cascades Implicated in Skin Homeostasis Maintenance

A decade ago, the importance of a complex network of serine protease cascades regulating skin homeostasis has begun to emerge. Matriptase, a transmembrane serine protease, has been shown to play an important role in inducing the proteolytic maturation of profilaggrin to filaggrin monomers via activation of other epidermal serine proteases, prostasin and furin (Fig. 3). The filaggrin monomers are further processed to individual hygroscopic amino acids that function as natural moisturizing factors contributing to the maintenance of a hydrated epidermis (MCGRATH *et al.* 2007). The discovery of the central role of matriptase in the signalling cascade leading to filaggrin processing has been greatly aided by the generation of a matriptase-deficient mouse model (LIST *et al.* 2002), demonstrating the importance of knock-out animal models in uncovering complex regulatory networks governing mammalian physiological processes *in vivo*.

Similarly, mounting evidence is linking members of the kallikrein-related peptidase (KLK) family to the regulation and maintenance of the desquamation process in the epidermal *stratum*

corneum layer. Several members of the KLK family are expressed as mRNA in healthy human epidermis, namely KLK1, KLK4, KLK5, KLK6, KLK7, KLK8, KLK9, KLK10, KLK11, KLK13 and KLK14 (KOMATSU *et al.* 2003). Importantly, it has been repeatedly demonstrated that KLK5 and KLK7 expression localizes to the *stratum granulosum* layer and both KLK5 and KLK7 together are able to cleave the corneodesmosomal proteins corneodesmosin, desmoglein 1 and desmocollin 1 (CAUBET *et al.* 2004). Proteolytic activity of KLK5 and KLK7 is linked to the acidic pH of *stratum corneum*, implying their role in corneodesmosome cleavage leading to desquamation of corneocytes in the *stratum corneum*, with possible activation via acidic pH. Since KLKs are expressed as inactive precursors that require proteolytic cleavage to become active enzymes, a multi-step protease cascade that governs the desquamation process has been postulated (CAUBET *et al.* 2004). Indeed, it has been demonstrated that KLK5 is able to activate other KLKs *in vitro*, implying a proteolytic activation cascade regulating corneocyte desquamation (BRATTSAND *et al.* 2005, STEFANSSON *et al.* 2006).

Furthermore, both KLK5 and KLK14 have been shown to be able to activate a transmembrane G-protein-coupled receptor, proteinase-activated receptor 2 (PAR2) *in vitro* (STEFANSSON *et al.* 2008). PAR2 is activated directly by protease cleavage of its N-terminal extracellular domain and is expressed in epidermal keratinocytes, thus colocalizing with both KLK14 and KLK5 *in vivo.* The ability of KLK5 and KLK14 to activate PAR2 suggests their direct involvement in epidermal inflammatory processes, since PAR2 activation induces the release of the pro-inflammatory factors thymic stromal lymphopoietin (TSLP), intercellular adhesion molecule 1, tumor necrosis factor alpha, and interleukin 8 (IL8), mediated by the nuclear factor-kappaB pathway (BRIOT *et al.* 2009).

However, the precise signalling and proteolytic cleavage cascade linking KLK and other epidermal proteases together and facilitating their role of skin homeostasis maintenance, inflammation and corneocyte desquamation *in vivo* remains unknown.

4.2.2. Netherton Syndrome as a Consequence of KLK Dysregulation

Netherton syndrome (NS) is an autosomal recessive disorder, characterized by severe congenital *ichthyosis* and disruption of the epidermal barrier that occurs in approximately one in 200 000 newborns (SMITH *et al.* 1995, BITOUN *et al.* 2002). Symptoms of NS vary in intensity from individual to individual and include scaly, peeling and itchy skin due to increased desquamation, dehydration, and persistent inflammatory *erythroderma*. Additionally, hair shaft defects termed "bamboo hair" (*trichorrhexis invaginata*) can be an occurring symptom in some NS patients (Fig. 4). While in some of the NS patients the condition improves with age, severe cases of NS can be lethal early in infancy.

It has been discovered that mutations in the gene *SPINK5* (Serine protease inhibitor Kazal-type 5) are the underlying factor of NS (CHAVANAS *et al.* 2000, FORTUGNO *et al.* 2011). The *SPINK5* gene encodes the serine protease inhibitor LEKTI (lympho-epithelial Kazal-type related inhibitor) that consists of 15 protease inhibitory domains. LEKTI is processed into

Figure 4. Netherton syndrome is a congenital ichthyosiform autosomal recessive disorder linked to LEKTI epidermal protease inhibitor deficiency due to mutations in *SPINK5*. Netherton syndrome (NS) patients displaying common symptoms of NS: exfoliating, scaly skin, inflammatory *erythroderma* (**A**-**D**) and "bamboo hair" hair shaft defects (*trichorrhexis invaginata*, **E**; adapted from HOVNANIAN *et al.* 2013).

fragments that are excreted in the epidermis and have been shown to inhibit KLK5, KLK7 and KLK14 (DERAISON *et al.* 2007). Thus, symptoms of NS have been linked to unregulated and therefore pathologically increased activity of serine proteases (including KLK5, KLK7 and KLK14). This discovery has been further substantiated by the fact that LEKTI-deficient mice display a phenotype very similar to NS: absence of *vibrissae*, *stratum corneum* detachment and severe dehydration that results in early postnatal lethality (Fig. 5; DESCARGUES *et al.* 2005, HEWETT *et al.* 2005, FURIO *et al.* 2015).

Indeed, a partial rescue of the lethal NS-like symptoms in LEKTI-deficient mice has been recently described (FURIO *et al.* 2015). Crossing LEKTI-deficient to KLK5-deficient mice led to prolonged survival of the resulting double-deficient offspring, accompanied by improved epidermal differentiation and lowered pro-inflammatory cytokine expression compared to the LEKTI-deficient mice. Therefore, dysregulation of the KLK proteolytic cascade in the epidermis is now assumed to be the underlying molecular mechanism of NS and could play a role in other epidermal diseases (MIYAI *et al.* 2014, MOLIN *et al.* 2015).

Finally, in our laboratory, we have confirmed the partial rescue of NS-like phenotype in LEKTI-deficient mice by the additional absence of KLK5 reported by FURIO *et al.* (2015).

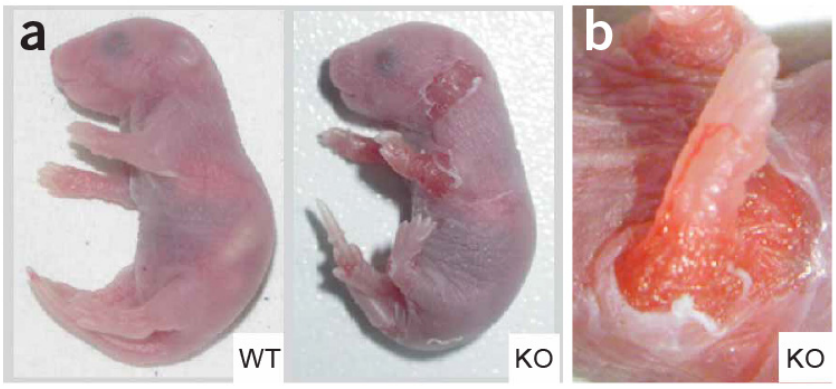

Figure 5. LEKTI-deficient mice phenocopy human Netherton syndrome (NS) patients. Mice with mutated *Spink5* (encoding the serine protease inhibitor LEKTI) display similar epidermal barrier defects as observed in NS patients and die within a few hours from birth (adapted from DESCARGUES *et al.* 2005).

Additionally, we have also prepared LEKTI and KLK7 double-deficient as well as LEKTI and KLK14 double-deficient mice (unpublished data). In contrast to the absence of KLK5 on the background of LEKTI-deficiency, both LEKTI and KLK7 double-deficient as well as LEKTI and KLK14 double-deficient mice do not show any significant differences in respect to survival and phenotype to LEKTI deficient mice. Importantly, we have also prepared a KLK5 and KLK7 double-deficient mouse strain (unpublished data). When crossed to LEKTI-deficient mice, the NS-like lethal phenotype is rescued almost completely, with the LEKTI, KLK5 and KLK7 triple-deficient mice surviving into adulthood, as opposed to LEKTI and KLK5 double-deficient mice reported by FURIO *et al.* (2015) where the rescue is only partial and the mice do not reach adulthood. Therefore, our results imply that KLK7 (and possibly other epidermal serine proteases) can be activated independently on KLK5. Furthermore, although the lethal phenotype is completely rescued, LEKTI, KLK5 and KLK7 triple-deficient mice still retain minor epidermal barrier defects, and interestingly, hair shaft defects very similar to the known symptom of NS, "bamboo hair" or *trichorrhexis invaginata* (manuscript submitted). We speculate therefore that KLK14 hyperactivity might be responsible for the phenotype in the LEKTI, KLK5 and KLK7 triple-deficient mice.

We have confirmed the findings of KOMATSU *et al.* (2003) and BHOGAL *et al.* (2014) regarding KLK14 expression being localized to the hair follicles by LacZ staining in Klk14$^{tm1a(KOMP)Wtsi}$ mice (RYDER et al., 2013, WEST et al. 2015) which express the LacZ reporter under endogenous *Klk14* promoter (Fig. 6 B, unpublished data). Additionally, mRNA expression analysis revealed an increase of KLK14 mRNA expression in the skin of wild type P5 – P8 (postnatal day 5 – postnatal day 8) pups, coinciding with the initial phase of fur growth in mouse pups (Fig. 6 A, unpublished data).

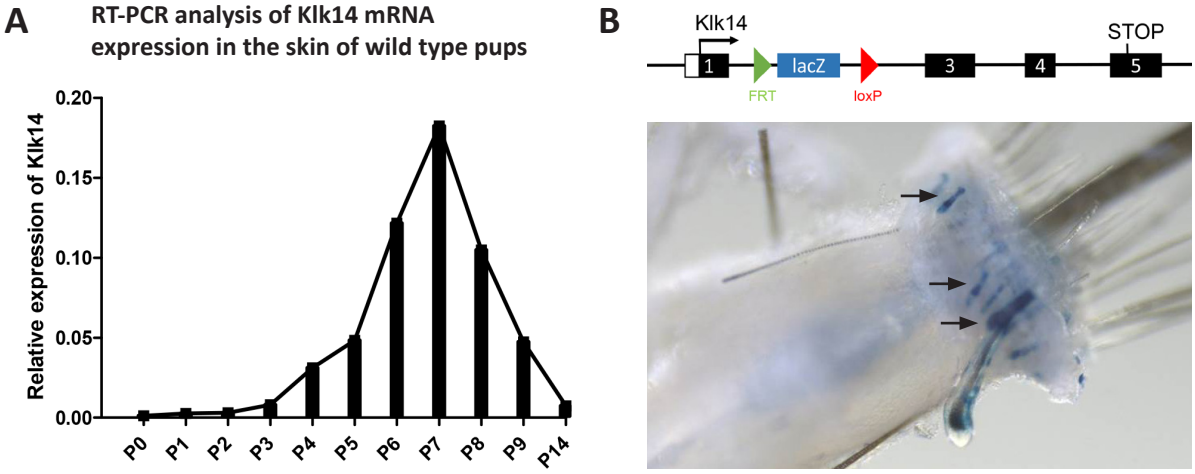

Figure 6. Klk14 expression in relation to fur growth in mice. *Klk14* mRNA expression in wild-type postnatal day 5 – postnatal day 8 (P5 – P8) pups increases coinciding with the initial phase of fur growth (**A**). LacZ reporter expression driven by the *Klk14* endogenous promoter in Klk14$^{tm1a(KOMP)Wtsi}$ mice reveals *Klk14* expression in hair follicles (**B**). Adapted from Zuzana Ileninova and Petr Kasparek (personal communication, unpublished data).

Thus, the expression pattern of KLK14 combined with our findings regarding the LEKTI, KLK5 and KLK7 triple-deficient mice support the assumption that KLK14 plays a role in NS. However, it is necessary to point out that all strains deficient in only one of the KLKs (KLK5, KLK7 and KLK14 deficient strains, respectively) appear to have no prominent epidermal phenotype. This is not the case for the KLK5 and KLK7 double-deficient mouse strain, where we observed a thickening of the *stratum corneum* along with later onset of fur growth. Therefore, it appears that there is at least a partial redundancy in KLK function within the epidermis. Consequently, we decided to prepare a KLK5 and KLK14 double-deficient mouse strain in order to explore the role of KLK14 in the context of LEKTI, KLK5 and KLK7 in the proteolytic cascades in the epidermis - not only underlying the symptoms of Netherton syndrome, but also under normal physiological conditions.

4.3. Application of Programmable Nucleases for the Generation of Mouse Models

The mouse (*Mus musculus*) has repeatedly proven itself as an indispensable tool for studying molecular interactions governing complex physiological processes in mammals, particularly for uncovering the underlying mechanisms of human disease. Recently, the development of programmable nucleases (PNs), namely transcription activator-like effector (TALE) nucleases and the clustered regularly interspaced short palindromic repeats (CRISPR)/Cas9 RNA-guided nuclease toolkit, has made the preparation of knock-out (KO) and transgenic animals more accessible. Formerly, the desired mutation had to be induced in murine embryonic stem cells (ESCs) which were then screened for positive targeting and subsequently added to wild type early-stage embryos in order to produce chimeric founder mice (DOW *et al.* 2012). Due to the recent and rapid advent of genome editing using PNs, this labor-intensive, lengthy and costly procedure is being partly replaced by a more streamlined approach: direct microinjection of PNs in the form of mRNA into one-cell stage mouse zygotes (WEFERS *et al.* 2013, FUJII *et al.* 2013, LI *et al.* 2014). PNs can be designed *in silico* to target specific sites within the genome and prepared by conventional molecular cloning methods (CERMAK *et al.* 2011, DOYLE *et al.* 2012, CONG *et al.* 2013). Additionally, PNs exhibit relatively high efficiency of cleavage, increasing the likelihood of obtaining positively targeted founder animals developed from microinjected zygotes.

The mechanisms of both target recognition and cleavage differ between the TALE and standard CRISPR/Cas9 nucleases (Fig. 7). While TALENs recognize their target through protein-DNA interaction, Cas9 binds guide RNA (gRNA) complementary to the target and is therefore reliant on RNA-DNA interaction for target recognition. Furthermore, TALENs act in pairs, requiring two TALE domains to bind to DNA sequences adjacent to the cleavage site (Left TALE and Right TALE, Fig. 7 A) in order to allow the C-terminal FokI cleavage domains to dimerize. In contrast, standard Cas9 is a standalone nuclease that does not require dimerization. Therefore, the two PN systems can differ in respect to off-target cleavage and cleavage efficiency (GAJ *et al.* 2013, HANECKOVA 2014).

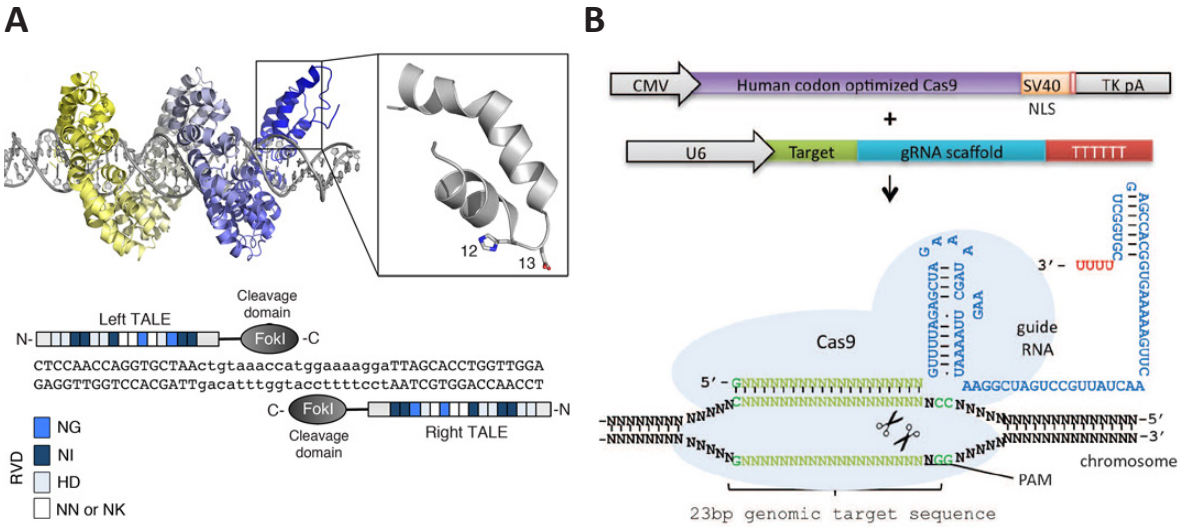

Figure 7. Mechanism of targeted DNA cleavage via TALE nucleases and CRISPR/Cas9 RNA-guided nuclease. The DNA-binding TALE domain consists of an array of repeats that contain repeat-variable di-residues (RVDs) specific to individual nucleobases (NG to thymine, NI to adenine, HD to cytosine and NN/NK to guanine). The TALE domain is fused to a C-terminal FokI nuclease domain. A pair of TALE nucleases are designed to bind to their target DNA so that the FokI nuclease domains are able to dimerize and cleave the target site (**A**). Cas9 is a RNA-guided nuclease that binds guide RNA (gRNA) and recognizes its target DNA by its complementarity to the bound gRNA and an adjacent 3 bp protospacer adjacent motif (PAM) sequence. Both Cas9 and gRNA can be expressed from the same vector (**B**; adapted from GAJ *et al.* 2013 and MALI *et al.* 2013).

Genome editing by PNs relies on endogenous DNA repair mechanisms of the targeted cell to induce the desired mutation. Upon PN cleavage, the resulting double-strand break (DSB) is likely repaired by the non-homologous end-joining (NHEJ) pathway, an error-prone DNA repair mechanism that often introduces indels of variable length resulting in frameshift and premature stop codons in the targeted gene. This way, a KO animal for the targeted gene can be prepared. Alternatively, if a template homologous to the sequences adjacent to the DSB is provided, the homology-directed repair pathway can be taken advantage of in order to introduce novel sequences into genomic DNA (WEFERS *et al.* 2013, KASPAREK *et al.* 2014).

We have successfully generated transgenic mouse strains containing TurboRFP and Blueflirt expression cassettes within the Rosa26 safe-harbor locus employing TALENs (KASPAREK *et al.* 2014) as well as a KLK5 and KLK7 double-deficient strain by introducing an indel mutation into *Klk7* on Klk5$^{tm2a(KOMP)Wtsi}$ (Klk5$^{-/-}$) background (manuscript submitted). Although KLK5, KLK7 and KLK14 deficient mouse strains have been available previously, intercrossing to obtain double- or triple-deficient strains is unfeasible due to the close proximity of the genes encoding the KLK family preventing recombination (Fig. 2; OLSSON *et al.* 2002, PAVLOPOPULOU *et al.* 2010). Genome editing using PNs therefore offers an alternative approach to generating mouse strains with multiple gene deficiencies where intercrossing is not feasible.

4.3.1. Surrogate Reporter Vectors for Verification of Programmable Nuclease Activity in Cell Culture

Although the generation of transgenic and knock-out mouse strains using microinjection of programmable nucleases (PNs) into zygotes is faster than the ESC approach, it remains a relatively labor-intensive and therefore costly process. To ensure that founders with the desired mutations are generated successfully, it is necessary for the PNs to cleave their target DNA with high efficiency. Therefore, assessing PN activity prior to their application *in vivo* is desirable.

For this purpose, several surrogate reporter systems that differ in reporter gene type and mechanism of activation that can be used for assessing PN activity and enriching for positively targeted cells in cell culture have been published (KIM *et al.* 2014, RAMAKRISHNA *et al.* 2014). We have developed our own surrogate reporter vector (pARv-RFP, Addgene plasmid # 60021) that enables verification of PN activity in cell culture (KASPAREK *et al.* 2014). The vector contains constitutively expressed GFP as well as inactive TurboRFP that serves as the reporter gene. The target site for PNs can be cloned into the TurboRFP multiple cloning site using EcoRV restriction digest and blunt-end cloning. Upon programmable nuclease cleavage, homology-directed repair leads to activation of the TurboRFP reporter gene (Fig. 8). Thus, PN activity can be assessed in cell culture by co-transfecting the cells with PN-expressing vectors in combination with pARv-RFP containing their respective target site. The transfected cells can be analyzed by fluorescence microscopy or FACS to determine the fluorescence intensity.

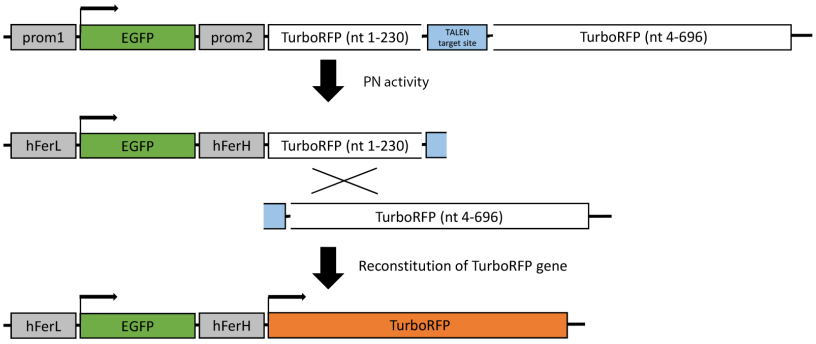

Figure 8. Mechanism of function of the pARv-RFP surrogate reporter vector. Reconstitution and activity of the TurboRFP reporter gene is dependent on programmable nuclease (PN) activity followed by double-strand break repair via the homologous recombination pathway (adapted from KASPAREK *et al.* 2014).

5. Materials and Methods

5.1. Design of Programmable Nucleases Targeting *Klk14*

The sequence of *Klk14* gene from the *Mus musculus* genome assembly, version GRCm38.p4 was obtained from the Ensembl database (FLICEK *et al.* 2014).

For designing TALE nuclease pairs targeting exons 2 and 3 of the *Klk14* gene, the online tool TAL Effector Nucleotide Targeter 2.0 (CERMAK *et al.* 2011, DOYLE *et al.* 2012) was used. Pairs with best score and low off-target site prediction were given preference. For exon 2, the repeat-variable di-residues (RVDs) NI HD NI NN NI NG NN NG NN NG HD HD NN NN NI NI HD NG HD HD (Klk14ex2 L) and NN HD HD HD NI NN NN HD HD HD NG NN HD NG NG NN HD NI NN NI (Klk14ex2 R) were selected. For exon 3, the RVDs NI NI NG NN NI HD HD NG HD NI NG NN HD NG NN HD NG (Klk14ex3 L) and NN HD NG HD NN NG HD HD HD NI NN HD HD NN HD NI HD HD (Klk14ex3 R) were selected. Both pairs of TALENs were chosen so that their predicted site of FokI dimerization and cleavage contains a restriction site: NcoI in case of the exon 2 TALEN pair, PstI in case of the exon 3 TALEN pair.

For designing gRNA sequences for the CRISPR/Cas9 programmable nuclease system targeting exon 2, the online tool provided by CONG *et al.* (2013) was used. The chosen targeted locus was selected to be identical to the locus for which the Klk14ex2 TALEN pair was designed. The gRNA target sites with the highest score were preferred and 4 gRNA target sites were selected: Klk14-2 gRNA #1 CCACACAGGAAGCGATGCCCAGG, Klk14-2 gRNA #2 GCTTGCAGAGCGACCTGCCATGG, Klk14-2 gRNA #3 AGTCCTGTTGTCAGATCAATGGG and Klk14-2 gRNA #4 GTGTCCGGAACTCCCAGCCATGG.

5.2. Generation of the TALE Nuclease Vectors

The TALEN pairs were assembled using the Golden Gate Cloning system (CERMAK *et al.* 2011). In the first assembly step, module plasmids containing the desired RVDs were combined with array plasmids and digested and ligated in a single reaction. For the ligation reaction, 65 ng of each RVD module plasmid, 65 ng of the respective array plasmid (pFUS_A for the first 10 RVDs, pFUS_B for the remaining RVDs), 0.5 µl of BsaI restriction enzyme (10 U/µl, Thermo Scientific™), 0.5 µl T4 DNA ligase (5 U/µl, Thermo Scientific™) and 1 µl T4 DNA ligase buffer (10X, Thermo Scientific™) were combined with H_2O to 10 µl total reaction volume. The reaction mix was incubated in a thermocycler (BIO-RAD T100™ Thermal Cycler) at 37 °C for 5 min and then at 16 °C for 10 min, repeated for 10 cycles, followed by heating to 50 °C for 5 min and subsequently to 80 °C for 5 min. After incubation, 0.25 µl of 25 mM ATP (Epicentre®) and 0.5 µl of Plasmid-Safe™ DNase (10 U/ul, Epicentre®) was added to the reaction mix. The reaction mix was incubated at 37 °C for 1 hour and heat-inactivated at 70 °C for 15 min. A 4 µl aliquot of the inactivated reaction mix (containing assembled RVD arrays in the pFUS array plasmids) was used to transform the competent *E. coli* strain XL1-Blue by using heat-shock at 42 °C for 1.5 min.

After incubating in 600 µl LB medium at 37 °C for 45 min, the transfected bacteria were resuspended in 100 µl volume of LB and plated on 19 mm LB agar plates containing 50 ng/µl spectinomycin and plated with 30 µl IPTG (100 mM, Thermo Scientific™) and 30 µl X-Gal (20 mg/mL, Thermo Scientific™) and incubated at 37 °C overnight.

Up to 6 white colonies were selected from each plate and screened for the correct RVD array using colony PCR. For the colony screening, the bacterial colonies were transferred from the plate into 40 µl LB medium and incubated for 1 hour at 37 °C. Primers as synthetic DNA oligonucleotides (Sigma Aldrich®) with the sequences TTGATGCCTGGCAGTTCCCT (Fu1 PCR8 F1) and CGAACCGAACAGGCTTATGT (Fu1 PCR8 R1) (CERMAK *et al.* 2011) were ordered and diluted to 10 µM concentration with H_2O. For the PCR reaction mix, 3 µl of the bacteria culture, 1 µl of each primer, 0.5 µl of deoxynucleotide mix (10 mM, Sigma Aldrich®), 2.5 µl DreamTaq polymerase buffer (10X, Thermo Scientific™) and 0.2 µl DreamTaq DNA Polymerase (5 U/µL, Thermo Scientific™) were combined with H_2O to 25 µl total reaction volume and incubated in a thermocycler at 95 °C for 10 min, for 34 cycles at 95 °C for 40 sec, 55 °C for 40 sec, 72 °C for 1 min 45 sec, followed by 72 °C final extension time for 3 min. The PCR mix was separated by gel electrophoresis on a 2 % agarose gel prepared from SeaKem® LE Agarose (Lonza) at 90V fixed voltage setting for 30 min. Positive colonies were then inoculated in 3 ml LB medium containing 50 µg/ml spectinomycin (pFUS_A and pFUS_B had spectinomycin resistance as selection marker) and incubated at 37 °C overnight.

The bacteria were centrifuged at 15000 g for 10 min at room temperature using a microcentrifuge (Eppendorf 5415R). The supernatant was discarded and plasmid DNA was isolated from the pellet using the GeneJET Plasmid Miniprep Kit (Thermo Scientific™) according to the protocol provided by the manufacturer. DNA concentration was measured using a UV-Vis Spectrophotometer (NanoDrop 2000c, Thermo Scientific™).

In the second assembly step, the partial RVD arrays contained in the pFUS_A and pFUS_B array plasmids that were generated in the first step were joined together with the last RVD and cloned into the modified ELD-KKR backbone plasmids (FLEMR *et al.* 2013, KASPAREK *et al.* 2014). For the ligation reaction, 75 ng of each array plasmid (pFUS_A containing the first 10 RVDs, pFUS_B containing the remaining RVDs), 75 ng of the last repeat plasmid (pLR with the respective RVD for each TALEN), 75 ng of backbone plasmid (ELD or KKR, one for each member of a TALEN pair), 0.5 µl of Esp3I restriction enzyme (10 U/µl, Thermo Scientific™), 0.5 µl T4 DNA ligase (5 U/µl, Thermo Scientific™) and 1 µl T4 DNA ligase buffer (10X, Thermo Scientific™) were combined with H_2O to 10 µl total reaction volume. The reaction mix was incubated in a thermocycler using the same setting as in the first step, the DNase treatment was omitted as recommended by the Golden Gate Cloning system protocol. The reaction mix was used to transform *E. coli* as described in the first assembly step, with spectinomycin being substituted with ampicillin (100 µg/ml) for selection of positive colonies on LB plates. White colonies were inoculated into 3 ml LB medium with ampicillin (100 µg/ml), and incubated at 37 °C overnight.

These bacteria with completely assembled TALE RVDs inside ELD and KKR backbone plasmids were again pelleted to isolate plasmid DNA as described in the first step.

The final assembled TALEN pairs for both target sites (Klk14ex2 L, R and Klk14ex3 L, R) were verified by restriction digest using the Kpn2I restriction enzyme. For the restriction digest, 0.5 µl of Kpn2I restriction enzyme (10 U/µl, Thermo Scientific™), 1.5 µl Tango Buffer (10X, Thermo Scientific™) and 400 ng to 600 ng of purified plasmid DNA were combined with H_2O to 15 µl total reaction volume and incubated at 37 °C for 2 hours. The digested plasmid DNA was separated by gel electrophoresis on a 2 % agarose gel prepared from SeaKem® LE Agarose (Lonza) at 90V fixed voltage setting for 40 min. Plasmids containing the Kpn2I digest pattern of fragments corresponding to a correct RVD array for each TALEN were selected.

5.3. Generation of the pX330 CRISPR/Cas9 Vectors

The pX330-U6-Chimeric_BB-CBh-hSpCas9 vector (pX330) expressing human codon-optimized SpCas9 nuclease and chimeric guide RNA (gRNA) under human U6 promoter was obtained from Feng Zhang via Addgene (CONG *et al.* 2013, Addgene plasmid # 42230).

Desalted and lyophilized synthetic DNA oligonucleotides (Sigma Aldrich®) were ordered and diluted to 100 µM concentration with H_2O (Table 1). The DNA oligonucleotides correspond to the coding strand (F) and complementary strand (R) that are coding the gRNA targeting the predicted site, with the addition of 5' CACC and AAAC overhangs (CONG *et al*. 2013). The protospacer adjacent motif (PAM) sequence is not included in the gRNA coding sequence (Fig. 9).

Table 1. Sequences of synthetic oligonucleotides ordered for generating gRNA targeting exon 2 of *Klk14*

Oligonucleotide	**Sequence**
Klk14-2 gRNA #1 F	5′ caccGCCACACAGGAAGCGATGCCC 3′
Klk14-2 gRNA #2 F	5′ caccGCTTGCAGAGCGACCTGCCA 3′
Klk14-2 gRNA #3 F	5′ caccAGTCCTGTTGTCAGATCAAT 3′
Klk14-2 gRNA #4 F	5′ caccGTGTCCGGAACTCCCAGCCA 3′
Klk14-2 gRNA #1 R	5′ aaacGGGCATCGCTTCCTGTGTGGC 3′
Klk14-2 gRNA #2 R	5′ aaacTGGCAGGTCGCTCTGCAAGC 3′
Klk14-2 gRNA #3 R	5′ aaacATTGATCTGACAACAGGACT 3′
Klk14-2 gRNA #4 R	5′ aaacTGGCTGGGAGTTCCGGACAC 3′

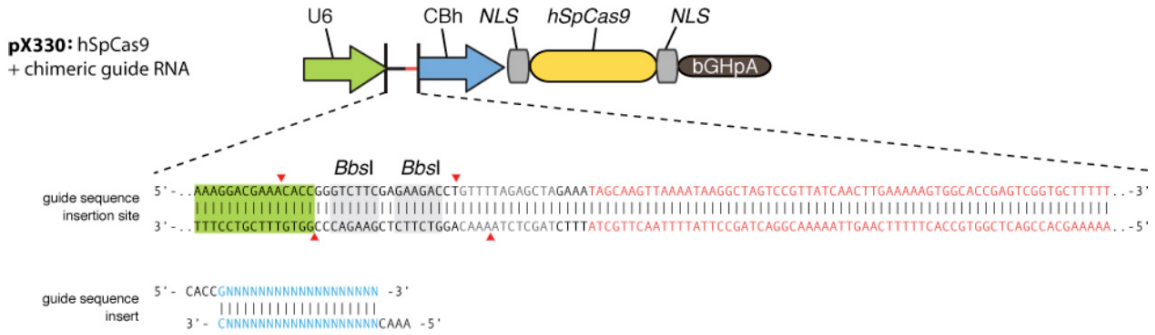

Figure 9. The pX330 vector. Generation of chimeric guide RNA by cloning a guide RNA (gRNA) oligonucleotide into the pX330 vector using overhangs generated by BbsI restriction digest of pX330 (adapted from CONG *et al.* (2013), Addgene plasmid # 42230).

5.3.1. Preparation of Linearized pX330 Vector and gRNA Oligonucleotides

The oligonucleotides (Table 1) were diluted to 10 mM concentration with H_2O and the corresponding F and R strands were annealed and phosphorylated. For the annealing, 5 µl of the F strand oligonucleotide (10 mM, Sigma Aldrich®), 5 µl of the R strand oligonucleotide (10 mM, Sigma Aldrich®) and 10 µl T4 DNA ligase reaction buffer (10X, New England BioLabs®) were combined with H_2O to 100 µl total reaction volume and incubated submerged in 5 liters of H_2O heated to 100 °C that was left to cool to room temperature overnight. For the phosphorylation reaction, 1 µl of the annealing reaction mix, 1 µl T4 polynucleotide kinase (10 U/µl, Thermo Scientific™) and 1 µl T4 DNA ligase reaction buffer (10X, New England BioLabs®) were combined with H_2O to 12 µl total reaction volume and incubated at 37 °C for 20 min and at 65 °C for 10 min.

The pX330 vector was linearized with the BbsI restriction enzyme to produce overhangs compatible with the gRNA oligonucleotides, dephosphorylated and purified prior to ligation.

For the restriction digest of pX330, 8 µg plasmid DNA, 2 µl BbsI restriction enzyme (10 U/µl, Thermo Scientific™) and 3 µl Green Buffer (10X, Thermo Scientific™) were combined with H_2O to 30 µl total reaction volume and incubated at 37 °C overnight. The reaction mix was inactivated at 65 °C for 20 min. The linearized pX330 plasmid DNA was purified using the GeneJET PCR Purification Kit (Thermo Scientific™) according to the protocol provided by the manufacturer and eluted in 25 µl H_2O.

For the dephosphorylation of pX330, 1.5 µl Antarctic Phosphatase (5 U/µl, New England BioLabs®) and 4 µl Antarctic Phosphatase buffer (10X, New England BioLabs®) were added to the linearized purified pX330 plasmid DNA, H_2O was added for 40 µl total reaction volume. The reaction mix was incubated at 37 °C for 15 min and at 70 °C for 5 min. The linearized dephosphorylated pX330 plasmid DNA was repeatedly purified using GeneJET PCR Purification Kit (Thermo Scientific™) according to the protocol provided by the manufacturer and eluted in 25 µl H_2O. DNA concentration was measured using a UV-Vis Spectrophotometer (NanoDrop 2000c, Thermo Scientific™).

5.3.2. Cloning of gRNA Oligonucleotides into the pX330 Backbone

Annealed and phosphorylated oligonucleotides Klk14-2 gRNA #1 – #5 were ligated individually into the linearized, dephosphorylated and purified pX330 vector. For the ligation reaction, 5 µl of the heat-inactivated phosphorylation mix containing the annealed oligonucleotides, 50 ng of linearized, dephosphorylated and purified plasmid DNA, 1.5 µl of T4 DNA ligase (5 U/µl, Thermo Scientific™) and 1.5 µl T4 DNA ligase buffer (10X, Thermo Scientific™) were combined with H_2O to 20 µl total reaction volume and incubated at 4 °C overnight. The ligation reaction mix was heat-inactivated at 65 °C for 10 min.

After inactivation, 4 µl of the reaction mix (containing gRNA sequences targeting exon 2 of *Klk14* in the pX330 backbone) was used to transform the competent *E. coli* strain XL1-Blue by using heat-shock at 42 °C for 1.5 min. After incubating in 600 µl LB medium at 37 °C for 45 min, the transfected bacteria were resuspended in 100 µl volume of LB, plated on 19 mm LB agar plates containing 100 ng/µl ampicillin and incubated at 37 °C overnight.

Correct integration of the gRNA oligonucleotide into the pX330 backbone was verified using colony PCR. Primers px330 F and px330 R supplied as synthetic DNA oligonucleotides (Sigma Aldrich®) with the sequences GACTATCATATGCTTACCGTAACTTG (px330 F) and TTATGTAACGGGTACCTCTAGAGC (px330 R) were ordered and diluted to 10 µM concentration with H_2O. The primers are flanking the gRNA oligonucleotide insertion site in the pX330 plasmid. Additionally, forward primers (Sigma Aldrich®) with annealing sites within the inserted gRNA oligonucleotides were ordered, with the sequences GCCACACAGGAAGCGATG (gRNA #1 Prim. F), TGCAGAGCGACCTGCC (gRNA #2 Prim. F), TCCGGAACTCCCAGCC (gRNA #4 Prim. F). For Klk14-2 gRNA #3, the forward synthetic oligonucleotide was used as forward primer for the colony PCR (Klk14-2 gRNA #3 F, for sequence see Table 1) and no additional forward primer was ordered.

Colony PCR was therefore performed with the px330 R primer as reverse primer and the respective gRNA forward primers or gRNA oligonucleotides for up to 4 colonies from each plate of cultivated transfected bacteria. The bacteria were transferred from the plate into 40 µl LB medium and incubated for 30 min at 37 °C. For the colony PCR, 3 µl of the bacteria culture, 1 µl of each primer, 0.5 µl of deoxynucleotide mix (10 mM, Sigma Aldrich®), 2.5 µl DreamTaq polymerase buffer (10X, Thermo Scientific™) and 0.2 µl DreamTaq DNA Polymerase (5 U/µL, Thermo Scientific™) were combined with H_2O to 25 µl total reaction volume and incubated in a thermocycler at 95 °C for 10 min, for 41 cycles at 95 °C for 30 sec, 50 °C for 30 sec, 72 °C for 40 sec, followed by 72 °C final extension time for 3 min. The PCR mix was separated by gel electrophoresis on a 2 % agarose gel prepared from SeaKem® LE Agarose (Lonza) at 90V fixed voltage setting for 30 min.

Colonies that produced a 200 bp long PCR fragment were presumed to contain the pX330 plasmid with correctly integrated gRNA oligonucleotide. Two positive colonies each were selected, inoculated in 3 ml LB medium containing 100 µg/ml ampicillin and incubated at 37 °C

overnight. The bacteria were centrifuged at 15000 g for 10 min at room temperature using a microcentrifuge (Eppendorf 5415R). The supernatant was discarded and plasmid DNA was isolated from the pellet using the GeneJET Plasmid Miniprep Kit (Thermo Scientific™) according to the protocol provided by the manufacturer. DNA concentration was measured using a UV-Vis Spectrophotometer (NanoDrop 2000c, Thermo Scientific™).

5.4. Generation of the pARv-RFP Surrogate Reporter Vectors

The surrogate activity reporter plasmid pARv-RFP was designed and prepared by us previously and is available on Addgene (KASPAREK *et al.* 2014, Addgene plasmid # 60021). pARv-RFP is based on the pVITRO2-MCS backbone (InvivoGen) and contains constitutively expressed enhanced green fluorescent protein (EGFP) PCR-amplified from the pEGFP-C1 plasmid (Clontech) under the human ferritin light chain composite promoter (hFerL) in the MCS1 site of pVITRO2-MCS. The reporter gene TurboRFP is under the control of the human ferritin heavy chain composite promoter (hFerH) in the MCS2 site.

As described in chapters 5.1. to 5.3, two target sites within the *Klk14* gene were selected and specific TALENs and gRNAs for CRISPR/Cas9 were designed and prepared. To test the prepared TALEN and CRISPR/Cas9 constructs, both sites (within exon 2 and exon 3 of *Klk14*, respectively) were prepared as synthetic oligonucleotides, annealed, and subcloned in the pARv-RFP vector.

Desalted and lyophilized synthetic DNA oligonucleotides (Sigma Aldrich®) were diluted to 100 µM concentration with H_2O. Complementary strands for both target sites were ordered (Table 2). The synthetic oligonucleotides were diluted to 10 mM concentration with H_2O, annealed, phosphorylated and ligated into the linearized and dephosphorylated pARv-RFP plasmid.

Table 2. Sequences of synthetic oligonucleotides ordered for cloning target sites into pARv-RFP.

Oligonucleotide	Sequence
Klk14 ex2 Target F	5′ ATTGGTGGCTACAGATGTGTCCGGAACTCCCAGCCATGGCAG GTCGCTCTGCAAGCAGGGCCTGGGCATCGCTTCCTGTGTGGA GGAGTCCTGTTGTCAGATCAATGGGTC 3′
Klk14 ex2 Target R	5′ GACCCATTGATCTGACAACAGGACTCCTCCACACAGGAAGCG ATGCCCAGGCCCTGCTTGCAGAGCGACCTGCCATGGCTGGGA GTTCCGGACACATCTGTAGCCACCAAT 3′
Klk14 ex3 Target F	5′ ATCTTAATGACCTCATGCTGCTGAAGCTGCAGAAAAAGGTGC GGCTGGGACGAGCAAGAT 3′
Klk14 ex3 Target R	5′ ATCTTGCTCGTCCCAGCCGCACCTTTTTCTGCAGCTTCAGCA GCATGAGGTCATTAAGAT 3′

For annealing and phosphorylation of the target oligonucleotides, the same protocol was used as for the gRNA oligonucleotides described in chapter 5.3.1. For linearization, dephosphorylation and purification of the pARv-RFP plasmid the same protocols was used as for the pX330 plasmid described in chapter 5.3.1. with the BbsI restriction enzyme (10 U/µl, Thermo Scientific™) and Green Buffer (10X, Thermo Scientific™) used to digest pX330 being substituted with the EcoRV (10 U/µl, Thermo Scientific™) restriction enzyme and Buffer Red (10X, Thermo Scientific™) to digest pARv-RFP.

Annealed and phosphorylated oligonucleotides Klk14 ex2 Target and Klk14 ex3 Target were ligated individually into the linearized, dephosphorylated and purified pARv-RFP vector. For the ligation reaction, 5 µl of the heat-inactivated phosphorylation mix containing the annealed oligonucleotides, 50 ng of linearized, dephosphorylated and purified plasmid DNA, 1.5 µl of T4 DNA ligase (5 U/µl, Thermo Scientific™), 1.5 µl T4 DNA ligase buffer (10X, Thermo Scientific™) and 2 µl polyethylene glycol 4000 (50 % w/v, Fermentas™) were combined with H_2O to 20 µl total reaction volume and incubated at 4 °C overnight. The ligation reaction mix was heat-inactivated at 65 °C for 10 min.

After inactivation, 4 µl of the inactivated reaction mix (containing the target site oligonucleotides in the TurboRFP reporter gene of pARv-RFP) was used to transform the competent *E. coli* strain XL1-Blue by using heat-shock at 42 °C for 1.5 min. After incubating in 600 µl LB medium at 37 °C for 45 min, the transfected bacteria were resuspended in 100 µl volume of LB, plated on 19 mm LB agar plates containing 100 µg/ml blasticidin S (Fast-Media® Blas Agar, InvivoGen) and incubated at 37 °C overnight.

5.4.1.Selection of pARv-RFP Vectors Containing the Target Site Inserts

Correct integration of the Klk14 ex2 Target oligonucleotide into the pARv-RFP backbone was verified using colony PCR. Primers Colony PARV F and Colony PARV R supplied as synthetic DNA oligonucleotides (Sigma Aldrich®) with the sequences TTGAGCGGAGCTAATTCTCG (Colony PARV F) and TCTCTCCCATGTGAAGCCC (Colony PARV R) were ordered and diluted to 10 µM concentration with H_2O. The primers were designed to amplify the target oligonucleotide insertion site, an empty pARv-RFP corresponds to a 691 bp long PCR product, pARv-RFP containing a correctly inserted Klk14 ex2 target corresponds to a longer 802 bp long product and contains an NcoI restriction site.

Six colonies of the transfected bacteria transferred from the plate into 40 µl LB medium and incubated for 1.5 hours at 37 °C. For the colony PCR, 3 µl of the bacteria culture, 1 µl of each primer, 0.5 µl of deoxynucleotide mix (10 mM, Sigma Aldrich®), 2.5 µl DreamTaq polymerase buffer (10X, Thermo Scientific™) and 0.2 µl DreamTaq DNA Polymerase (5 U/µL, Thermo Scientific™) were combined with H_2O to 25 µl total reaction volume and incubated in a thermocycler at 95 °C for 10 min, for 34 cycles at 95 °C for 40 sec, 53 °C for 30 sec, 72 °C for 1 min, followed by 72 °C final extension time for 3 min. The PCR mix was separated by gel electrophoresis on a 2 % agarose gel prepared from SeaKem® LE Agarose (Lonza) at 90V fixed voltage setting for 30 min.

Colonies that produced an 802 bp long PCR fragment were presumed to contain the pARv-RFP plasmid with correctly integrated oligonucleotide. Correct insertion was also confirmed by NcoI digest of the PCR product. Colonies containing the Klk14 ex2 Target oligonucleotide correctly integrated in the pARv-RFP backbone were then inoculated in 3 ml Fast-Media® Blas TB (InvivoGen) liquid medium containing 100 µg/ml blasticidin S and incubated at 37 °C overnight.

The bacteria cultures were centrifuged at 15000 g for 10 min at room temperature using a microcentrifuge (Eppendorf 5415R). The supernatant was discarded and plasmid DNA was isolated from the pellet using the GeneJET Plasmid Miniprep Kit (Thermo Scientific™) according to the protocol provided by the manufacturer. DNA concentration was measured using a UV-Vis Spectrophotometer (NanoDrop 2000c, Thermo Scientific™).

Correct integration of the Klk14 ex3 Target oligonucleotide into the pARv-RFP backbone was verified using Sanger sequencing. Three colonies of the bacteria transfected with the ligation mix containing the Klk14 ex3 Target oligonucleotide were selected from the plate. The colonies were transferred directly into 3 ml Fast-Media® Blas TB (InvivoGen) liquid medium containing 100 µg/ml blasticidin S and incubated at 37 °C overnight. The bacteria cultures were again pelleted, plasmid DNA was isolated and its concentration was measured as described above. The sequencing was performed by the company SEQme and the samples were prepared according to their protocol. The primer used for sequencing was supplied as synthetic DNA oligonucleotides by Sigma Aldrich® with the sequence GCTGGAAGTCATTTTTGGAA, and was designed to anneal 438 bp upstream from the Klk14 ex3 Target insertion site. 500 ng of purified plasmid DNA from each selected colony and 2.5 µl of the primer (diluted to 10 µM with H_2O) were combined with H_2O to 10 µl total volume in a 1.5 ml micro tube (Sarstedt), and sealed with Parafilm M® (Bemis®). Sequencing data obtained from SEQme was analyzed using SeqMan Pro and SeqBuilder software by DNASTAR®. One out of the three colonies analyzed was found to contain the correctly inserted oligonucleotide within the pARv-RFP backbone.

5.5. Verification of Programmable Nuclease Activity in Cell Culture

The fibroblast NIH3T3 (ATCC® CRL-1658™) cell line (derived from *Mus musculus* embryonic tissue) was obtained. The cells were cultured in high glucose Dulbecco's Modified Eagle Medium (DMEM; 500 ml, Sigma Aldrich®) supplemented with 5 ml Penicillin-Streptomycin solution (10,000 U/mL of each antibiotic, Thermo Scientific™), and 50 ml fetal bovine serum (Thermo Scientific™) at 37 °C in a Forma™ 310 Direct Heat CO_2 incubator (Thermo Scientific™) at 5 % CO_2 concentration. For transfection, Lipofectamine® LTX Reagent with PLUS™ Reagent (Invitrogen™) was used and the cells were transfected according to the protocol provided by the manufacturer. The cells were cultured to 50-60 % confluence on CellBIND® 48 Well Clear Multiple Well Plates (Corning®) in 500 µl medium prior to transfection. For each well, 500 ng of DNA was used: 200 ng of each TALEN plasmid (Klk14ex2 L, R and Klk14ex3 L, R) was combined with 100 ng of the respective pARv-RFP plasmid containing the target site (Klk14 ex2 Target and Klk14 ex3 Target). For the CRISPR/Cas9 programmable nucleases targeting exon 2 of *Klk14*,

400 ng of the pX330 plasmid containing each gRNA (Klk14-2 gRNA #1 - #5) was combined with the pARv-RFP plasmid containing the Klk14 ex2 Target site (Table 3).

For each well, 0.5 µl PLUS™ Reagent and 500 ng plasmid DNA were added to serum-free and antibiotics-free DMEM in a 1.5 ml micro tube and incubated for 10 min at room temperature. 1.2 µl Lipofectamine® LTX Reagent was added to each transfection mix, incubated for 20 min at room temperature and added to the well. The cells were incubated for 4 days at 37 °C prior to further analysis. The transfected cells were imaged with an inverted fluorescence microscope (OLYMPUS IX521) in combination with a Hg fluorescence light source, CCD camera (OLYMPUS DP70), an objective with 40X magnification and the imaging software DP Controller (OLYMPUS, v. 2.2.1.227). Green fluorescence was observed through a GFP filter, red fluorescence through a PI filter.

Table 3. Transfection of murine fibroblast NIH3T3 cells with pX330 CRISPR/Cas9, TALEN, and pARv-RFP vectors. Amount of DNA for each plasmid and well added up to 500 ng DNA total per well.

Well	Plasmids transfected	DNA
Well 1:	pARv-RFP/Klk14 ex2 Target Klk14-2 L TALEN Klk14-2 R TALEN	100 ng 200 ng 200 ng
Well 2:	pARv-RFP/Klk14 ex2 Target pX330/Klk14-2 gRNA #1	100 ng 400 ng
Well 3:	pARv-RFP/Klk14 ex2 Target pX330/Klk14-2 gRNA #2	100 ng 400 ng
Well 4:	pARv-RFP/Klk14 ex2 Target pX330/Klk14-2 gRNA #3	100 ng 400 ng
Well 5:	pARv-RFP/Klk14 ex2 Target pX330/Klk14-2 gRNA #4	100 ng 400 ng
Well 6:	pARv-RFP/Klk14 ex2 Target pX330/Klk14-2 gRNA #5	100 ng 400 ng
Well 7:	pARv-RFP/Klk14 ex3 Target Klk14-3 L TALEN Klk14-3 R TALEN	100 ng 200 ng 200 ng
Well 8:	pARv-RFP/Klk14 ex2 Target Klk14-3 L TALEN Klk14-3 R TALEN	100 ng 200 ng 200 ng

5.6. Preparation of *Klk14* Exon 3 TALEN mRNA and Microinjection

5.6.1. *In Vitro* Transcription and Polyadenylation

The TALEN plasmid Klk14ex3 L and R were linearized using the NotI restriction enzyme, followed by *in vitro* transcription from the T7 RNA polymerase promoter and polyadenylation.

For NotI restriction digest, 10 µg purified plasmid DNA in H_2O, 2 µl NotI restriction enzyme (10 U/µl, Thermo Scientific™) and 3 µl Buffer O (10X, Thermo Scientific™) were combined with H_2O to 30 µl total reaction volume and incubated at 37 °C overnight. The reaction mix was inactivated at 80 °C for 20 min.

The linearized plasmid DNA was purified using the GeneJET PCR Purification Kit (Thermo Scientific™) according to the protocol provided by the manufacturer and eluted in 30 µl H_2O. DNA concentration was measured using a UV-Vis Spectrophotometer (NanoDrop 2000c, Thermo Scientific™).

In vitro transcription was performed using the mMESSAGE mMACHINE® T7 transcription kit (Ambion™) according to the protocol supplied by the manufacturer. For the *in vitro* transcription reaction, 400 ng of purified linearized plasmid DNA, 5 µl NTP/CAP solution (2X), 1 µl reaction buffer (10X) and 1 µl enzyme mix were combined with H_2O to 10 µl total reaction volume and incubated at 37 °C for 1 hour. 0.5 µl TURBO DNase (2 U/µL, Ambion™) was added to the reaction mix and incubated at 37 °C for 15 min.

Polyadenylation was performed using the Poly(A) tailing kit (Ambion™). For the polyadenylation reaction, 18 µl of H_2O, 10 µl of E-PAP buffer (10X), 5 µl MnCl2 (25 mM) and 5 µl ATP (10 mM) were added to the DNase-treated *in vitro* transcription reaction mix. 0.5 µl of the reaction mix was removed to serve as control prior to adding 2 µl of E-PAP enzyme and incubating the reaction mix at 37 °C for 1 hour. The resulting polyadenylated TALEN mRNA was purified using the RNeasy® Mini Kit (Qiagen), eluted in 50 µl H_2O, and verified by gel electrophoresis on a 1 % agarose gel prepared from SeaKem® LE Agarose (Lonza) at 90V fixed voltage setting for 45 min. RNA concentration was measured using a UV-Vis Spectrophotometer (NanoDrop 2000c, Thermo Scientific™). mRNA for the left and right TALEN (Klk14ex3 L and R) was pooled 1:1 to a concentration of 40 ng/µl for microinjection.

5.6.2. Microinjection of TALEN mRNA into $Klk5^{tm2a(KOMP)Wtsi}$ ($Klk5^{-/-}$) Zygotes

The mice were housed by the Animal Facility of the Institute of Molecular Genetics of the ASCR in specific-pathogen-free housing conditions. The microinjections and subsequent zygote transfers were performed in the Transgenic and Archiving Module of the Czech Center for Phenogenomics.

$Klk5^{tm2a(KOMP)Wtsi}$ ($Klk5^{-/-}$) females aged 3-5 weeks were superovulated intraperitoneally with 5 I. U. Folligon® (Intervet), followed by 5 I. U. human chorionic gonadotropin hormone (hCG; Sigma) after 48 hours. The females were mated with $Klk5^{tm2a(KOMP)Wtsi}$ ($Klk5^{-/-}$) males and checked for plugs. Zygotes were isolated from the oviducts of mated and plugged females 20 hours after

administration of hCG. The zygotes were suspended in M2 medium and treated with hyaluronidase to remove the cumulus cells prior to microinjection. The TALEN mRNA (40 ng/µl) was microinjected into the cytoplasm and male pronuclei. The manipulated zygotes were transferred into the oviducts of CD-1 foster mothers (20-25 zygotes per female) housed with sterile males prior to zygote transfer.

The generation, housing of mice, and in vivo experiments were in compliance with national and institutional guidelines and approved by the Animal Care Committee of the Institute of Molecular Genetics of the ASCR.

5.7. Genomic DNA Isolation and Genotyping

5.7.1 Genomic DNA Isolation

Genomic DNA was isolated from tail biopsies using QuickExtract™ DNA extraction solution (Epicentre). For DNA isolation, 50 µl of the solution were added to the tissue, incubated at 55 °C for 30 min and inactivated at 95 °C for 5 min.

5.7.2. Genotyping for *Klk14* by PCR and PstI Digest

Primers Klk14-3 F and Klk14-3 R supplied as synthetic DNA oligonucleotides (Sigma Aldrich®) with the sequences ACAAGAGGCCACAAAATGCT (Klk14-3 F) and ACCCAGGAGTCCAACATCAG (Klk14-3 R) were ordered and diluted to 10 µM concentration with H_2O. The primers were flanking the TALEN target site within the *Klk14* exon 3 containing a PstI restriction site immediately adjacent to the cleavage site.

For the PCR reaction, 3 µl of the QuickExtract™ DNA extraction reaction mix, 1 µl of each primer (Klk14-3 F, R), 0.5 µl of deoxynucleotide mix (10 mM, Sigma Aldrich®), 2.5 µl DreamTaq polymerase buffer (10X, Thermo Scientific™) and 0.2 µl DreamTaq DNA Polymerase (5 U/µL, Thermo Scientific™) were combined with H_2O to 25 µl total reaction volume and incubated in a thermocycler at 95 °C for 3 min, for 41 cycles at 95 °C for 30 sec, 61 °C for 30 sec, 72 °C for 40 sec, followed by 72 °C final extension time for 3 min.

The resulting PCR product was digested by the PstI restriction enzyme (10 U/µl, Thermo Scientific™) by directly adding 0.8 µl of PstI to 10 µl of the PCR mix and incubating it at 37 °C overnight. The reaction mix was separated by gel electrophoresis on a 2 % agarose gel prepared from SeaKem® LE Agarose (Lonza) at 90V fixed voltage setting for 45 min.

5.7.3. Genotyping for *Klk14* by Sanger Sequencing

For genotyping, the PCR product obtained by the PCR protocol described in chapter 5.7.2 was purified, cloned into pGEM®-T Easy vector (Promega) and sequenced using Sanger sequencing.

The PCR reaction mix was purified using the GeneJET PCR Purification Kit (Thermo Scientific™) according to the protocol provided by the manufacturer. DNA concentration was measured using a UV-Vis Spectrophotometer (NanoDrop 2000c, Thermo Scientific™).

The purified PCR fragments were eluted in 30 µl H_2O and cloned into the pGEM®-T Easy vector (Promega). For the ligation reaction, 50 ng of the vector, 24.1 ng of the Klk14 exon 3 PCR product from each selected founder, 1.5 µl T4 DNA ligase (5 U/µl, Thermo Scientific™) and 10 µl ligation buffer (2X, Promega) were combined with H_2O to 20 µl total reaction volume, incubated at room temperature for 4 hours and inactivated at 65 °C for 10 min. 4 µl of the inactivated reaction mix was used to transform the competent *E. coli* strain XL1-Blue by using heat-shock at 42 °C for 1.5 min. After incubating in 600 µl LB medium at 37 °C for 45 min, the transfected bacteria were resuspended in 100 µl volume of LB and plated on 19 mm LB agar plates containing 100 µg/ml ampicillin and plated with 30 µl IPTG (100 mM, Thermo Scientific™) and 30 µl X-Gal (20 mg/mL, Thermo Scientific™) and incubated at 37 °C overnight.

Up to 12 white colonies were selected from each plate and screened for the insertion of a non-wt PCR product into the pGEM®-T Easy vector using colony PCR and PstI digest. The bacteria were transferred from the plate into 40 µl LB medium and incubated for 1 hour at 37 °C. For the colony PCR screen, 3 µl of the bacteria culture, 1 µl of each primer (Klk14-3 F, R), 0.5 µl of deoxynucleotide mix (10 mM, Sigma Aldrich®), 2.5 µl DreamTaq polymerase buffer (10X, Thermo Scientific™) and 0.2 µl DreamTaq DNA Polymerase (5 U/µL, Thermo Scientific™) were combined with H_2O to 25 µl total reaction volume and incubated in a thermocycler at 95 °C for 10 min, for 41 cycles at 95 °C for 30 sec, 61 °C for 30 sec, 72 °C for 40 sec, followed by 72 °C final extension time for 3 min. The resulting PCR product was digested by the PstI restriction enzyme as described before.

Up to 4 colonies identified as containing shortened or undigested PCR products within the pGEM®-T Easy vector were inoculated in 3 ml LB medium containing ampicillin (100 µg/ml) and incubated at 37 °C overnight. The bacteria cultures were centrifuged at 15000 g for 10 min at room temperature using a microcentrifuge (Eppendorf 5415R). The supernatant was discarded and plasmid DNA was isolated from the pellet using the GeneJET Plasmid Miniprep Kit (Thermo Scientific™) according to the protocol provided by the manufacturer. DNA concentration was measured using a UV-Vis Spectrophotometer (NanoDrop 2000c, Thermo Scientific™).

The sequencing was performed by the company SEQme and the samples were prepared according to their protocol. The primers used for sequencing were Klk14-3 F, Klk14-3 R and M13R (sequence CAGGAAACAGCTATGACC, annealed 130 bp downstream of the cloning site on the pGEM®-T Easy vector). For sequencing, 500 ng of purified plasmid DNA from each selected colony and 2.5 µl of the primer (diluted to 10 µM with H2O) were combined with H_2O to 10 µl

total volume in a 1.5 ml micro tube (Sarstedt) and sealed with Parafilm M® (Bemis®). Sequencing data obtained from SEQme was analyzed using BioEdit, SeqMan Pro and SeqBuilder software by DNASTAR®. The sequences obtained were manually aligned to the *Mus musculus* genome assembly version GRCm38.p4, gene *Klk14*.

5.7.4. Genotyping for *Klk5*

For *Klk5* genotyping, Primers supplied as synthetic DNA oligonucleotides (Sigma Aldrich®) with the sequences TGCATGGTTTGGTATGGAGC (Klk5KO F) and TCCATTCTAGAGC-CAATCCTAAATTC (Klk5KO R) were ordered and diluted to 10 µM concentration with H_2O. The wild-type allele results in a 262 bp long PCR product, while the tm2a allele results in a 231 bp long PCR product.

For the PCR reaction, 3 µl QuickExtract™ DNA extraction solution (Epicentre) reaction mix, 1 µl of each primer (Klk5KO F, R), 0.5 µl of deoxynucleotide mix (10 mM, Sigma Aldrich®), 2.5 µl DreamTaq polymerase buffer (10X, Thermo Scientific™) and 0.2 µl DreamTaq DNA Polymerase (5 U/µL, Thermo Scientific™) were combined with H_2O to 25 µl total reaction volume and incubated in a thermocycler at 95 °C for 3 min, for 34 cycles at 95 °C for 20 sec, 63 °C for 25 sec, 72 °C for 30 sec, followed by 72 °C final extension time for 3 min. The PCR reaction mix was separated by gel electrophoresis on a 2 % agarose gel prepared from SeaKem® LE Agarose (Lonza) at 90V fixed voltage setting for 45 min.

5.8. Analysis of Postnatal Day 8 (P8) Pups

Litters obtained from $Klk5^{+/-}Klk14^{del69/+}$ x $Klk5^{+/-}Klk14^{del69/+}$ and $Klk5^{+/-}Klk14^{del5/+}$ x $Klk5^{+/-}Klk14^{del5/+}$ (het x het) breeding pairs were analyzed at the postnatal day 8 (P8) stage. The pups were genotyped for *Klk5* and *Klk14* as described in chapter 5.7. The mice were weighed (Sartorius M-power scales) and anesthetized by injection of 70 µl 30 % Zoletil 100 (Virbac, 50 mg/mL Tiletamine and 50 mg/mL Zolazepam) in PBS intraperitoneally. Photographs of head, extremities, ventral and dorsal skin (at 0.63X magnification), *vibrissae* (at 1.25X magnification) and tail (at 5X magnification) were obtained with a brightfield stereo microscope (OLYMPUS SZX10) and CDC camera (OLYMPUS DP72). Tail biopsies were performed for genomic DNA isolation and genotyping. Tissue samples of dorsal skin (1 cm^2, above the tail) were isolated for RNA and protein isolation and stored at -80 °C. Whole pups were fixed in 50 ml 4 % formaldehyde (p.a. grade, PENTA s.r.o.) in PBS for 24 hours and moved to 50 ml 75 % ethanol (p.a. grade, VWR®).

The pups were transferred to the Histopathology Unit of the Czech Center for Phenogenomics for whole-body paraffin-embedding, sectioning and staining. Whole P8 pups were embedded in paraffin blocks, cut to 2 µm sections with a microtome in the sagittal plane, fixed to glass slides and stained with hematoxylin and eosin (H&E). The slides with sections were incubated at 55 °C overnight, re-hydrated in a descending alcohol series (xylene, isopropyl alcohol, 96 % ethanol, 70 % ethanol, H_2O), immersed in Harris hematoxylin solution, washed with H_2O and

immersed in eosin solution. The stained samples were dehydrated in an ascending alcohol series (70 % ethanol, 96 % ethanol, absolute ethanol, isopropyl alcohol and absolute ethanol 1:1, isopropyl alcohol and xylene) and mounted with DPX mounting medium under a coverslip. The sections were analyzed and images obtained using the a Zeiss Axioscan Z1 (Carl Zeiss AG) at 20x and 10x magnification.

5.8.1 Isolation of RNA from Dorsal Skin, Reverse Transcription and cDNA Analysis

Dorsal skin samples obtained from postnatal day 8 (P8) pups born in $Klk5^{+/-}Klk14^{del69/+}$ x $Klk5^{+/-}Klk14^{del69/+}$ and $Klk5^{+/-}Klk14^{del5/+}$ x $Klk5^{+/-}Klk14^{del5/+}$ (het x het) breedings were analyzed. The samples were frozen and crushed with a pestle in liquid nitrogen. Acid guanidinium thiocyanate-phenol-chloroform extraction of RNA and proteins was performed for each sample. For the extraction, 600 µl TRI Reagent® (Sigma Aldrich®) was added to the crushed tissue, the mixture was incubated for 10 min at room temperature and centrifuged with a microcentrifuge (Eppendorf™ 5424 R) at 12000 g for 10 min. The supernatant was transferred to a 1.5 ml micro tube (Sarstedt) containing 120 µl chloroform (p.a. grade, PENTA s.r.o.), shaken repeatedly and centrifuged at 12000 g for 15 min. 200-300 µl of the aqueous phase (containing the RNA fraction) and 300-400 µl of the organic phase (containing the protein fraction) were removed to separate 1.5 ml micro tubes. 180 µl of absolute ethanol (VWR®) was added to the protein fraction, the sample was centrifuged at 2000 g for 5 min, the supernatant was moved to a fresh 1.5 ml micro tube and the samples were stored at -20 °C. 300 µl of isopropyl alcohol (p. a. grade, Lachner) was added to the RNA fraction and the samples were centrifuged at 12000 g for 15 min. The supernatant was discarded and the pellet was washed in 600 µl 75 % ethanol (p.a. grade, PENTA s.r.o.). The samples were centrifuged at 7500 g for 5 min, the supernatant was discarded and the pellet was dried and dissolved in 50 µl H_2O by incubating the sample at 55 °C for 15 min. RNA concentration was measured using a UV-Vis Spectrophotometer (NanoDrop 2000c, Thermo Scientific™). RNA quality was verified by gel electrophoresis on a 1 % agarose gel prepared from prepared from SeaKem® LE Agarose (Lonza) at 90V fixed voltage setting for 45 min.

In vitro reverse transcription using M-MLV reverse transcriptase (Promega) was performed for each RNA sample. For the reverse transcription reaction, 600 ng of RNA, 2 µl of M-MLV RT 5X buffer (Promega), 1 µl oligo(dT)15 primer (35µM, Promega), 0.5 µl of deoxynucleotide mix (10 mM, Sigma Aldrich®), 0.5 µl RNasin® ribonuclease inhibitor (20–40 u/µl, Promega) and 0.5 µl M-MLV reverse transcriptase (200 u/µl, Promega) were combined with H_2O to 20 µl total reaction volume. The reaction mix was incubated in a thermocycler (BIO-RAD T100™ Thermal Cycler) at 42 °C for 1 hour. 60 µl H_2O were added to each reaction.

The cDNA obtained from RNA isolated from dorsal skin samples of P8 pups was screened for *Klk14* cDNA via PCR using a series of primers annealing to exon 3 and exon 4 of *Klk14* mRNA. Primers supplied as synthetic DNA oligonucleotides (Sigma Aldrich®) with the sequences CCTGGGCAAGCACAACAT (Klk14 cDNA 4F) and ACTGCAGAGCAGTGGGGTAC (Klk14 cDNA 4R) were ordered and diluted to 10 µM concentration with H_2O. For the PCR,

3 µl of cDNA from each dorsal skin sample, 1 µl of each primer, 0.5 µl of deoxynucleotide mix (10 mM, Sigma Aldrich®), 2.5 µl DreamTaq polymerase buffer (10X, Thermo Scientific™) and 0.2 µl DreamTaq DNA Polymerase (5 U/µL, Thermo Scientific™) were combined with H_2O to 25 µl total reaction volume and incubated in a thermocycler at 95 °C for 3 min, for 41 cycles at 95 °C for 30 sec, 61 °C for 30 sec, 72 °C for 1 min, followed by 72 °C final extension time for 3 min. The PCR reaction mix was separated by gel electrophoresis on 2 % and 1 % agarose gels (SeaKem® LE Agarose, Lonza) at 90V fixed voltage setting for 45 min. Sanger Sequencing of the PCR products was performed directly from the purified PCR products. The sequencing was performed by the company SEQme and the samples were prepared according to their protocol. The primers used for sequencing were the same that were used for PCR. For sequencing, 100 ng of purified PCR product and 2.5 µl of the primer (diluted to 10 µM with H_2O) were combined with H_2O to 10 µl total volume in a 1.5 ml micro tube (Sarstedt) and sealed with Parafilm M® (Bemis®).

Sequencing data obtained from SEQme was analyzed using BioEdit, SeqMan Pro and SeqBuilder software by DNASTAR®. The sequences obtained were manually aligned to the *Klk14* transcript sequence (ID ENSMUST00000056329.6) obtained from the Ensembl database (FLICEK *et al.* 2014).

5.9. Statistical Analysis

Statistical analysis of Mendelian ratios and sex distribution was performed using the Chi square test and GraphPad Prism software (version 7).

6. Results

6.1. Generation of TALENs and CRISPR/Cas9 targeting *Klk14*

6.1.1. Design and Preparation of TALEN Vectors

Transcription activator-like effector nucleases (TALENs) targeting exon 2 and exon 3 of *Klk14* (Fig. 10 A) were designed and assembled using the Golden Gate Cloning system as described by CERMAK *et al.* and KASPAREK *et al.* The target sites in exon 2 and exon 3 were selected to include a restriction site within the cleavage site of the respective TALEN pairs; NcoI in the case of exon 2 and PstI in the case of exon 3. Indel mutations introduced by double-strand break (DSB) following programmable nuclease (PN) cleavage and subsequent repair by the non-homologous end-joining (NHEJ) pathway were expected to disrupt the restriction sites; thus enabling the screening for successfully targeted founder mice by restriction fragment length polymorphism (RFLP).

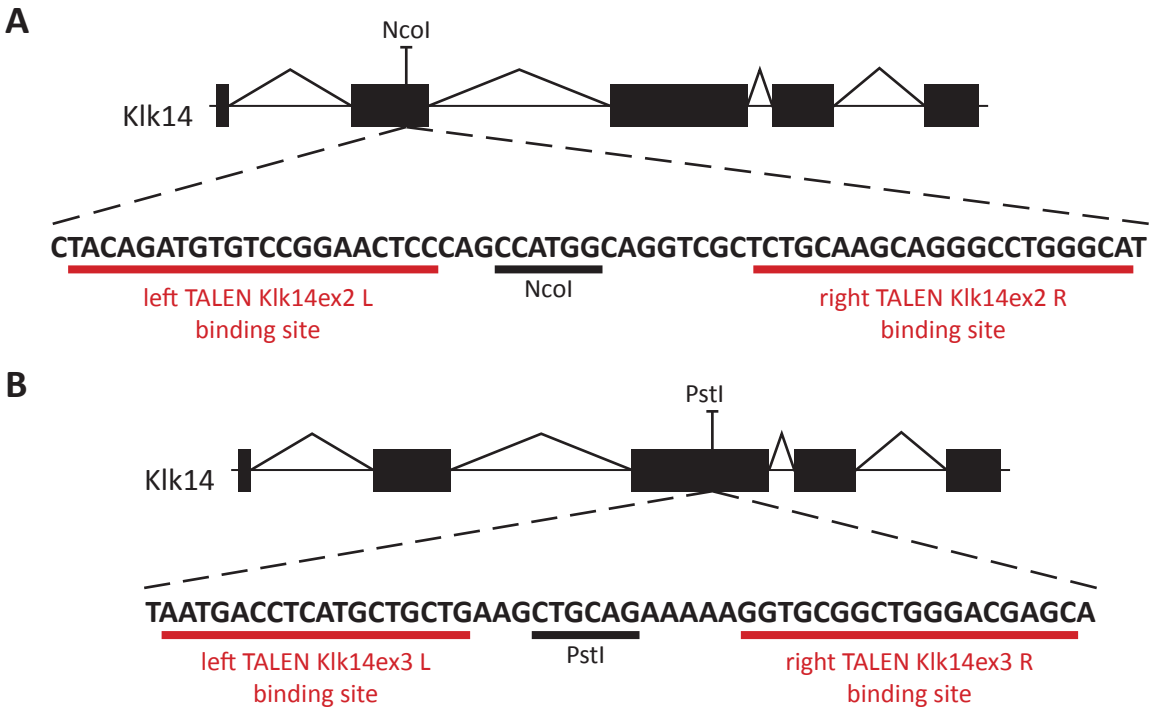

Figure 10. TALENs targeting *Klk14*. Two pairs of TALENs targeting exon 2 (**A**) and exon 3 (**B**) of *Klk14* were designed so as to include a restriction site immediately at the cleavage site.

The repeat-variable di-residue (RVD) arrays (Table 4) were assembled in a two-step cloning process and verified by RFLP using Kpn2I. A Kpn2I restriction site is present in HD RVDs in positions 2 to 10 in the arrays assembled in the first cloning step in vectors pFUS_A and pFUS_B, thus no restriction site was expected in HD repeats in positions 1, 11 and in the final repeat in the completed TALE RVD array.

Kpn2I digest of the completed TALEN vectors produced the expected pattern of bands in very few of the clones obtained from the second assembly step (Fig. 11 A, B, D); most of the clones contained incomplete RVD arrays. After the activity of both TALEN pairs along with the

Table 4. RVD arrays of the TALENs.

	1	2	3	4	5	6	7	8	9	10	11	12	13	14	15	16	17	18	19	20
Klk14ex2 L	NI	HD	NI	NN	NI	NG	NN	NG	NN	NG	HD	HD	NN	NN	NI	NI	HD	NG	HD	HD
Klk14ex2 R	NN	HD	HD	HD	NI	NN	NN	HD	HD	HD	NG	NN	HD	NG	NG	NN	HD	NI	NN	NI
Klk14ex3 L	NI	NI	NG	NN	NI	HD	HD	NG	HD	NI	NG	NN	HD	NG	NN	HD	NG			
Klk14ex3 R	NN	HD	NG	HD	NN	NG	HD	HD	HD	NI	NN	HD	HD	NN	HD	NI	HD	HD		

CRISPR/Cas9 constructs targeting exon 2 of *Klk14* (chapter 6.2.) was confirmed in cell culture, the TALEN pair targeting exon 3 of *Klk14* (Klk14ex3 L, R) was selected for *Klk14* targeting in mice. mRNA of each TALEN was prepared from the linearized vectors by *in vitro* transcription from the T7 RNA polymerase promoter and polyadenylation.

The quality of resulting mRNA was verified by gel electrophoresis. mRNA of both TALENs produced discrete bands indicative of intact, undegraded RNA. *In vitro* polyadenylation resulted in longer products compared to untreated mRNA, indicating successful generation of polyadenylated TALEN mRNA (Fig. 11 C).

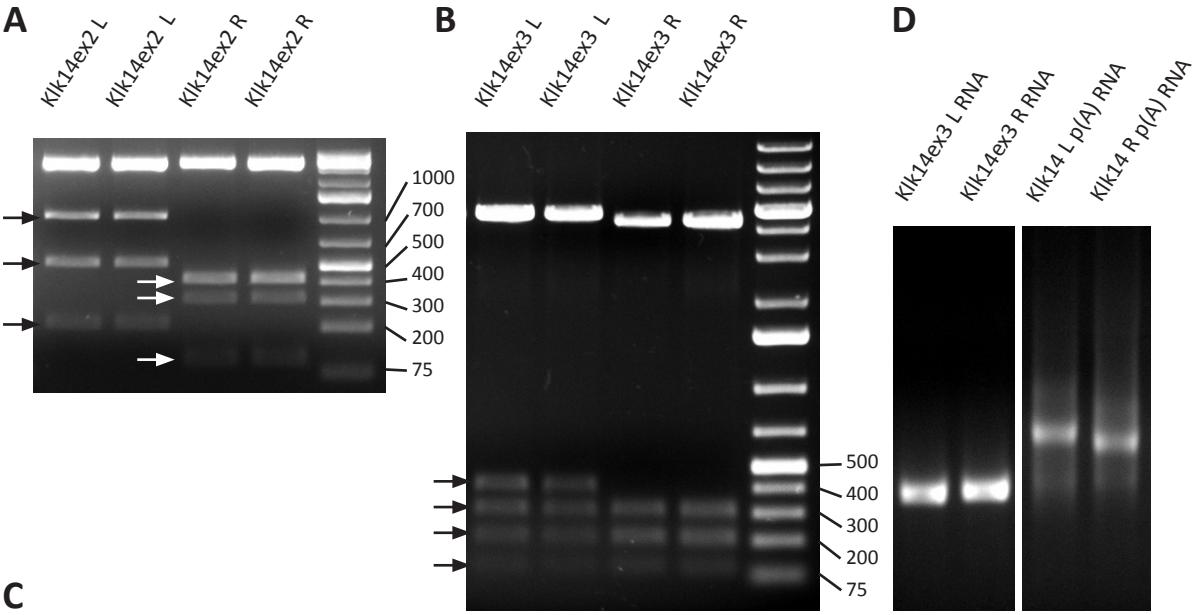

Figure 11. RFLP analysis of prepared TALENs targeting exon 2 (Klk14ex2 L, R) and exon 3 (Klk14ex3 L, R) of *Klk14* and quality control of Klk14ex3 R, L TALEN RNA. Kpn2I digest of the completely assembled TALEN vectors (**A**,**B**) resulted in composition of bands (black and white arrows) that corresponded to HD repeat distribution in the RVDs of the individual TALENs (**D**). RNA obtained from *in vitro* transcription of the TALEN pair targeting exon 3 of *Klk14* (Klk14ex3 L RNA, Klk14ex3 R RNA) as well as RNA after *in vitro* polyadenylation (Klk14ex3 L p(A) RNA, Klk14ex3 R p(A)RNA) appeared as uniform bands indicative of intact, undegraded RNA (**C**).

6.1.2. Design and Preparation of CRISPR/Cas9 Vectors

Additionally to the TALENs targeting exon 2 of *Klk14*, guide RNA (gRNA) was designed to target the same locus as the TALEN pair and cloned into the pX330-U6-Chimeric_BB-CBh-hSpCas9 (pX330) vector. The pX330 vector expresses the human codon-optimized SpCas9 nuclease and enables insertion of custom oligonucleotides to form chimeric guide RNA (gRNA) expressed under the human U6 promoter. The gRNA is bound by SpCas9 nuclease and facilitates cleavage of a DNA sequence complementary to the gRNA. Four different synthetic oligonucleotides coding for gRNAs targeting exon 2 of *Klk14* were cloned into pX330 (Fig. 12).

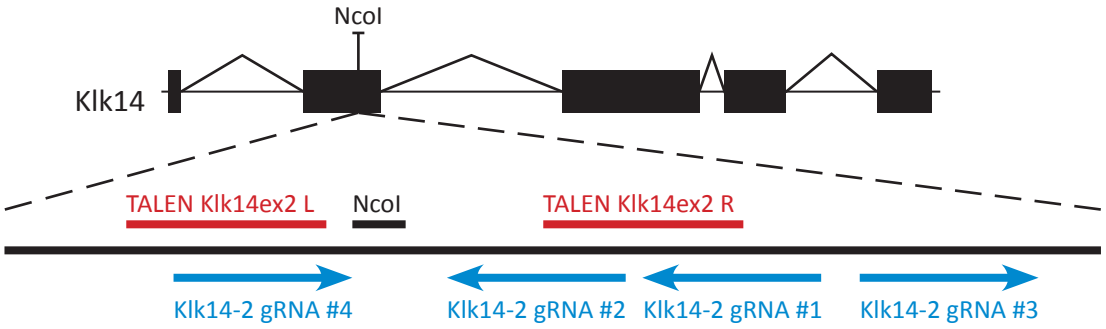

Figure 12. Guide RNAs (gRNAs) targeting exon 2 of *Klk14*. Four gRNAs were designed and cloned into the pX330 vector. The gRNAs are complementary to sequences in the same locus as the Klk14ex2 L, R TALEN pair (red bars). The blue arrows indicate the SpCas9 cleavage sites corresponding to each gRNA.

The correct integration of the gRNA oligonucleotides into pX330 was confirmed by colony PCR, with the forward primer annealing to the gRNA oligonucleotide and the reverse primer annealing downstream of the U6 terminator (Fig. 13 A). All bacterial colonies (4 for each respective gRNA) transfected with the ligation reaction mix were found to contain correctly integrated gRNA oligonucleotides (Fig. 13 B).

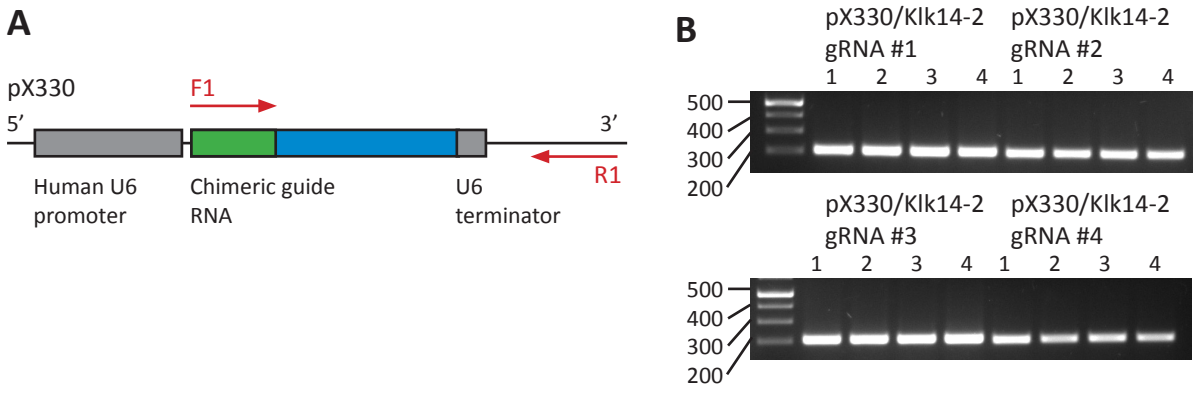

Figure 13. Confirmation of correct integration of gRNA nucleotides into pX330. For colony PCR, a forward primer annealing to the inserted gRNA oligonucleotide (F1, red arrow) in combination with a reverse primer annealing downstream of the chimeric gRNA U6 terminator (F2, red arrow) were used (**A**). Out of 4 colonies analyzed for each gRNA, all were confirmed to contain the inserted gRNA oligonucleotide (**B**).

6.2. Activity of Programmable Nucleases in Cell Culture

In order to verify if the TALENs and CRISPR/Cas9 gRNAs are capable of inducing cleavage of their respective target DNA sequences, we prepared surrogate reporter system (pARv-RFP) vectors containing target sequences for both exon 2 and exon 3 specific programmable nucleases (PNs). The target sequences were cloned as synthetic oligonucleotides into the multiple cloning site within the TurboRFP reporter gene. For TALENs and CRISPR/Cas9 gRNAs targeting exon 2, a 111 bp synthetic oligonucleotide target sequence was cloned into pARv-RFP. The sequence contains a NcoI restriction site as well as all the targeted sequences for both TALENs and CRISPR/Cas9 gRNAs. (Fig. 14 A).

The resulting pARv-RFP/Klk14 ex2 Target vectors were analysed by RFLP in order to confirm correct integration of the oligonucleotide. The construct was digested separately with HindIII and NcoI restriction enzymes. In one out of the six vector constructs analyzed, the NcoI digest

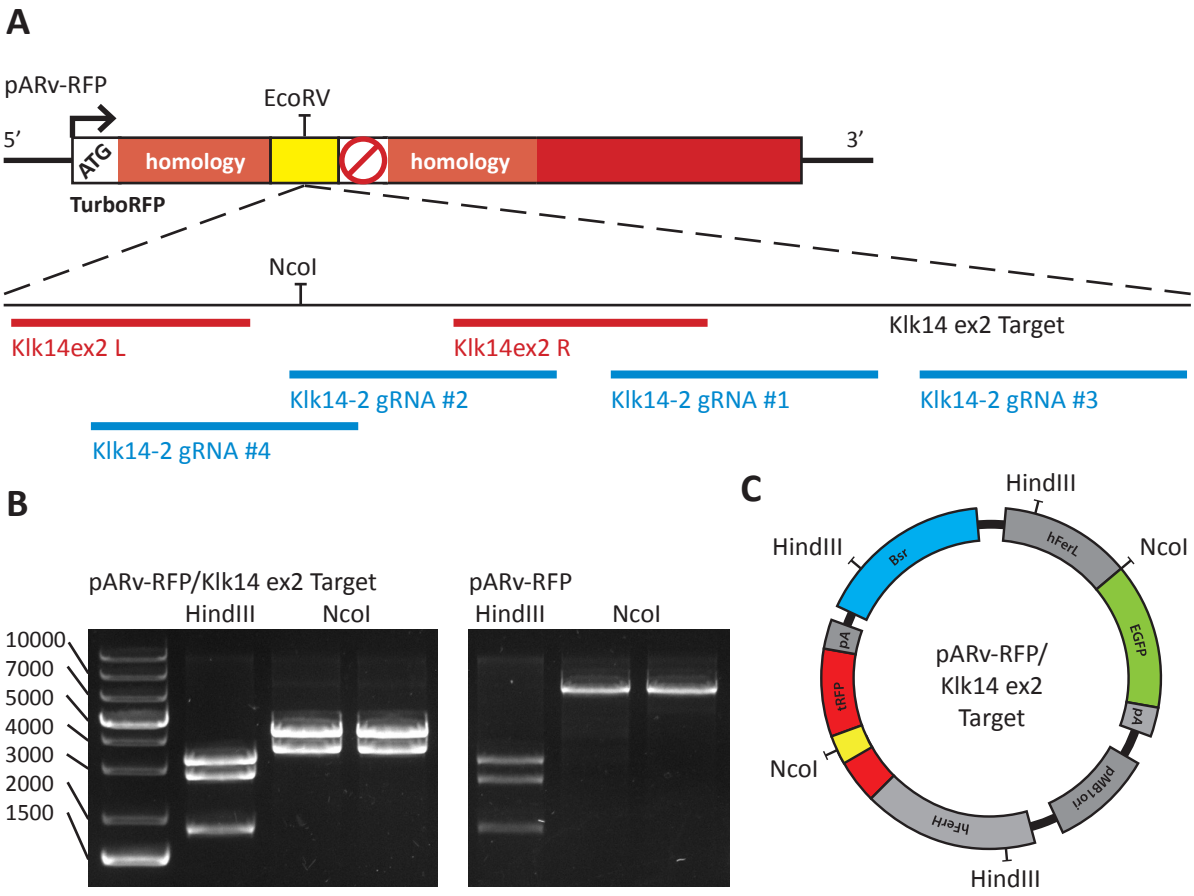

Figure 14. The pARv-RFP surrogate reporter vector for TALENs targeting exon 2 of *Klk14*. The 111 bp long synthetic oligonucleotide (Klk14 ex2 Target) was cloned into the multiple cloning site (**A**, yellow) of the TurboRFP reporter gene via an EcoRV restriction site (**A**). Klk14 ex2 Target contains sequences targeted by the Klk14ex2 L, R TALEN pair (**A**, red underscore) as well as Klk14-2 gRNAs #1 - #4 (**A**, blue underscore). Digest with the HindIII and NcoI restriction enzymes was used to confirm the correct integration of the Klk14 ex2 Target into pARv-RFP. pARv-RFP with integrated Klk14 ex2 Target contains an additional NcoI site and produces two fragments when digested with NcoI, compared to the empty pARv-TRFP vector with only one NcoI site (**B**, **C**).

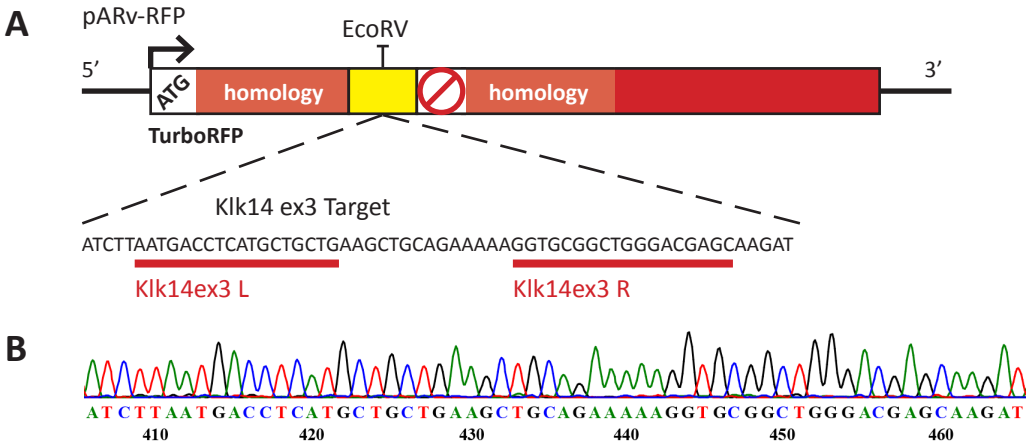

Figure 15. The pARv-RFP surrogate reporter vector for TALENs targeting exon 3 of *Klk14*. The 60 bp long synthetic oligonucleotide (Klk14 ex3 Target) was cloned into the multiple cloning site (**A**, yellow) of the TurboRFP reporter gene via an EcoRV restriction site (**A**). The Klk14 ex3 Target oligonucleotide contains the sequence targeted by the Klk14ex3 L, R TALEN pair (**A**, red underscore). Correct integration of the Klk14 ex3 Target oligonucleotide was confirmed via Sanger sequencing (**B**).

produced two fragments, indicating the insertion of the Klk14 ex2 Target within pARv-RFP by the presence of an additional NcoI site in comparison to the empty pARv-RFP vector (Fig. 14 B, C). For the TALEN pair targeting exon 3, a 60 bp synthetic oligonucleotide target sequence was cloned into pARv-RFP (Fig. 15 A). The resulting pARv-RFP/Klk14 ex3 Target vectors were analysed by Sanger sequencing in order to confirm correct integration of the oligonucleotide (Fig. 15 B).

Murine fibroblast NIH3T3 cells were co-transfected with the PN vectors in combination with a pARv-RFP vector containing their respective target sequence using lipofection. For each well of the 48 well culture plate, 500 ng of DNA was used for transfection: 200 ng of each TALEN vector (Klk14ex2 L, R and Klk14ex3 L, R) was combined with 100 ng of the respective pARv-RFP plasmid containing the target site (Klk14 ex2 Target and Klk14 ex3 Target). In the case of CRISPR/Cas9 PNs, 400 ng of the pX330 plasmid containing each gRNA was combined with 100 ng pARv-RFP plasmid containing the Klk14 ex2 Target site (Fig. 16 A). Additionally, the TALEN pair targeting exon 3 was combined with the pARv-RFP reporter vector containing the exon 2 target oligonucleotide to serve as negative control. The transfected cells were incubated for 4 days and subsequently examined under a fluorescence microscope (Fig. 16 B). The pARv-RFP reporter vector contains constitutively expressed EGFP, and green fluorescence was observed in all transfected wells. More importantly, red fluorescence indicating actively transcribed TurboRFP reporter gene was observed in all transfected wells with the exception of the negative control, where no red fluorescence could be observed. The intensity of red fluorescence seemed to show a slight variability of intensity, with the wells transfected with TALENs displaying a higher level of TurboRFP expression when compared to the wells transfected with the CRISPR/Cas9 vectors. Consequently, the TALEN pair targeting exon 3 of *Klk14* was chosen for targeting *Klk14* in mice and mRNA for microinjection was prepared (Chapter 6.1.1.).

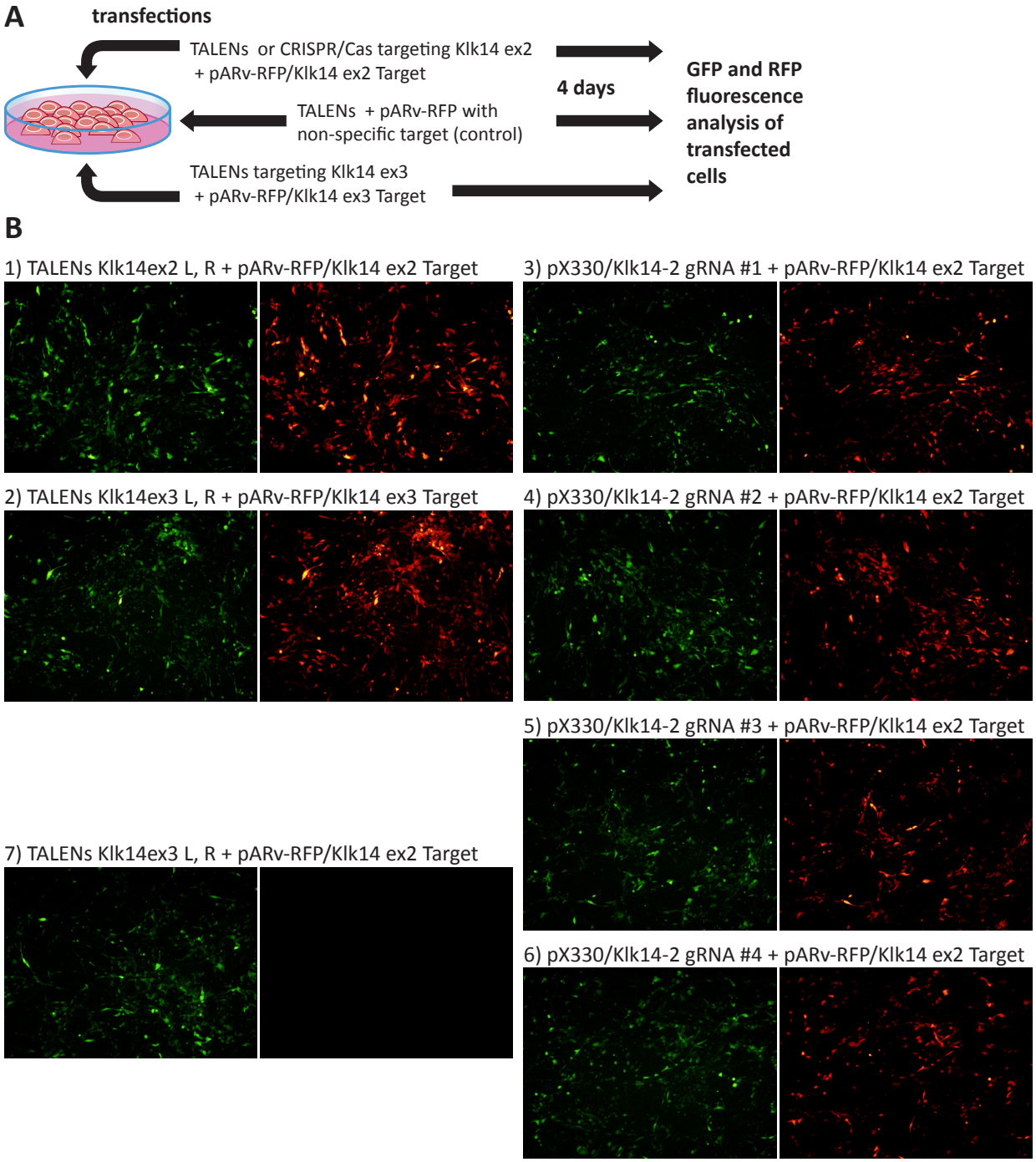

Figure 16. Murine fibroblast NIH3T3 cells were transfected with programmable nuclease (PN) vectors in combination with pARv-RFP containing their respective target sequences and examined for GFP and RFP fluorescence intensity. TALEN pairs Klk14ex2 L, R and Klk14ex3 L, R and CRISPR/Cas9 vectors pX330/Klk14-2 gRNA #1 – #4 were paired with their respective pARv-RFP reporter vectors containing the exon 2 and exon 3 target oligonucleotides and co-transfected into murine fibroblast NIH3T3 cells (**A**). After 4 days, red and green fluorescence was observed under a fluorescence microscope (**B**). Green fluorescence was comparable in all transfected wells (**B** 1 – 7). Red fluorescence varied in intensity, with the cells transfected with TALENs showing a slight increase (**B** 1, 2) when compared to cells transfected with CRISPR/Cas9 (**B** 3 – 6). No red fluorescence was observed in the negative control, containing the TALENs for exon 3 in combination with the pARv-RFP containing the exon 2 target (**B** 7).

6.3. Selection of Founders

Four litters of pups were born to the CD-1 foster mothers. All pups displayed black fur typical for the C57Bl/6NCrl strain, indicating that all pups developed from the implanted Klk5$^{tm2a(KOMP)Wtsi}$ (Klk5$^{-/-}$) microinjected embryos. Genomic DNA was isolated from all founders after weaning and analyzed by PCR and restriction fragment length polymorphism (RFLP) via PstI digest. The PCR product from the wild-type *Klk14* allele was expected to be 482 bp and produce 292 bp and 190 bp fragments upon cleavage. If the allele was successfully targeted by TALENs and subsequently repaired via error-prone NHEJ (LIEBER *et al.* 2010), the PCR product obtained from the mutated allele was expected to differ in length from the wild-type allele PCR product. Additionally, if the PstI recognition site within the TALEN cleavage site was mutated, the PCR product obtained from the mutated allele was expected to resist PstI cleavage.

RFLP analysis of genomic DNA obtained from tail biopsies revealed that in 16 out of 34 mice the PstI site located within the *Klk14* exon 2 TALEN target site (Fig. 17 B) has been disrupted (Fig. 17 A). Founder 2 did not produce a digested product, implying that the PstI site has been disrupted on both alleles of *Klk14*. Founder 24 had a significantly shortened undigested PCR product, indicating the presence of a longer deletion in the TALEN target site, which was subsequently confirmed by sequencing (Fig. 17 D). All 16 positive founders identified by RFLP analysis were additionally analyzed by Sanger sequencing of the targeted locus and a range of mutations within the targeted locus was identified (Fig. 17 D). The type of mutations identified were to a large extent short deletions ranging from 2 bp to 24 bp, in some cases combined with insertions or substitutions of individual base pairs. Two of the mutations identified were more extensive: a 69 bp deletion and a 108 bp deletion combined with a 23 bp insertion that was found to be present in two of the founder mice. Interestingly, in 4 mice (founders 2, 18, 20, 24; Fig. 17 A, D) sequencing of the targeted locus revealed multiple different mutations present in one individual. In our case, 4 out of 16 founder mice with mutations in the targeted locus were identified as mosaic according to the analysis of genomic DNA obtained from tail biopsies (Fig. 17 C). Founders with long deletions, deletions resulting in a frameshift in the KLK14 coding sequence, or both types of mutation were selected for breeding. Founders 20 and 24 did not transmit the long deletion of 108 bp to their offspring. Founder 20 transmitted only the 2 bp deletion, while founder 24 transmitted only the 69 bp deletion. Founders 22 and 30 were chosen for breeding due to their 2 bp and 5 bp deletions leading to frameshift, and both founders transmitted the mutations to their offspring.

6.4. Establishment of KLK5 and KLK14 Double-deficient Mouse Strains

Two distinct strains were derived from the founder mice obtained from microinjection of TALEN mRNA targeting exon 3 of *Klk14*. Each strain was determined to carry a different mutation within exon 3 of *Klk14* that was likely to result in non-functional KLK14. Both mutations were induced on Klk5$^{tm2a(KOMP)Wtsi}$ (Klk5$^{-/-}$) background, thus resulting in strains that were expected to be double-deficient for both KLK5 and KLK14.

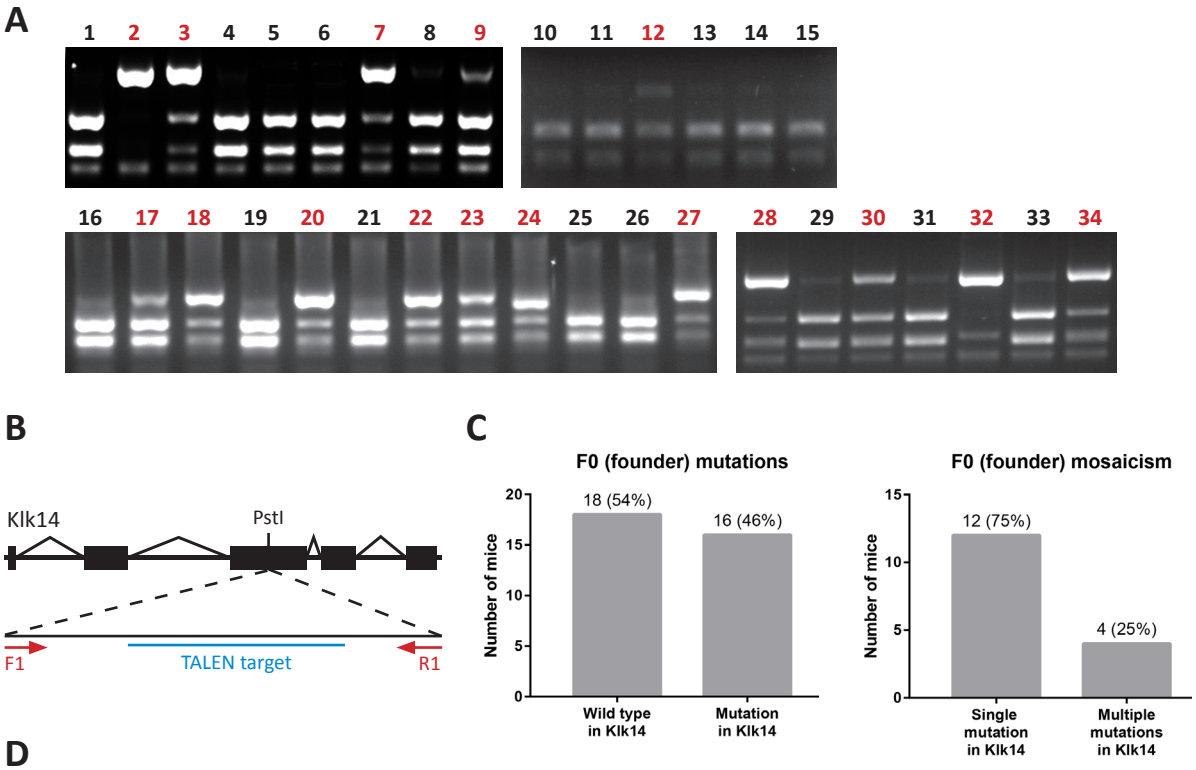

D

```
WT   ATCAACCCCAGGCCCACGATAATGACCTCATGCTGCTGAAGCTGCAGAAAAAGGTGCGGCTGGGACGAGCAGTGAAGACCATCTCTG
2A   ATCAACCCCAGGCCCACGATAATGACCTCATGCTGCTGAAG----------GTGCGGCTGGGACGAGCAGTGAAGACCATCTCTG  -12
2B   ATCAACCCCAGGCCCACGATAATGACCTCATGCTGCTGAAGCTG----------CGGCTGGGACGAGCAGTGAAGACCATCTCTG  -12
3    ATCAACCCCAGGCCCACGATAATGACCTCATGCTGCTTAAGCTGCAG---CAGGTGCGGCTGGGACGAGCAGTGAAGACCATCTCTG  -3
7    ATCAACCCCAGGCCCACGATAATGACCTCATGCTGCTGAAGCTG---------GTGCGGCTGGGACGAGCAGTGAAGACCATCTCTG  -9
12   ATCAACCCCAGGCCCACGATAATGACCTCATGCT------------------------GCTGGGACGAGCAGTGAAGACCATCTCTG  -24
17   ATCAACCCCAGGCCCACGATAATGACCTCATGCTGCTGAAG------AAAAAGGTGCGGCTGGGACGAGCAGTGAAGACCATCTCTG  -6
18A  ATCAACCCCAGGCCCACGATAATGACCTCATGCTGCTGAAG----------GTGCGGCTGGGACGAGCAGTGAAGACCATCTCTG  -12
18B  ATCAACCCCAGGCCCACGATAATGACCTCATGC------------------------GGCTGGGACGAGCAGTGAAGACCATCTCTG  -24
20A  ATCAACCCCAGGCCCACGATAATGACCTCATGCTGCTGAAGCTGG---AAAAGGTGCGGCTGGGACGAGCAGTGAAGACCATCTCTG  -3, C/A > G
20B  ATCAACCCCAGGCCCACGATAATGACCTCATGCTGCTGAAGCTG--GAAAAAGGTGCGGCTGGGACGAGCAGTGAAGACCATCTCTG  -2
22   ATCAACCCCAGGCCCACGATAATGACCTCATGCTGCTGAAGCTC--GAAAAAGGTGCGGCTGGGACGAGCAGTGAAGACCATCTCTG  -2, G/A > C
23   ATCAACCCCAGGCCCACGATAATGACCTCATGCTGCT---------GAAAAAGGTGCGGCTGGGACGAGCAGTGAAGACCATCTCTG  -9
27   ATCAACCCCAGGCCCACGATAATGACCTCATGCTGCT---------GAAAAAGGTGCGGCTGGGACGAGCAGTGAAGACCATCTCTG  -9
28   ATCAACCCCAGGCCCACGATAATGACCTCATGCTGCTGAA------GAAAAAGGTGCGGCTGGGACGAGCAGTGAAGACCATCTCTG  -6
30   ATCAACCCCAGGCCCACGATAATGACCTCATGCTGCTGAAG-----AAAAAAGGTGCGGCTGGGACGAGCAGTGAAGACCATCTCTG  -5  C/G > A
32   ATCAACCCCAGGCCCACGATAATGACCTCATGCTGCTGAA---------AAAGGTGCGGCTGGGACGAGCAGTGAAGACCATCTCTG  -9
34   ATCAACCCCAGGCCCACGATAATGACCTCATGCTGCTGAAG------AAAAAGGTGCGGCTGGGACGAGCAGTGAAGACCATCTCTG  -6

WT   AGGTGCCACATCCCCAGTATCAACCCCAGG...TGCTGAAGCTGCAGAAAAAGGTGCGGCTGGGACGAGCAGTGAAGACCATCTCTG
24A  AGGTGC-------------------------...------------------------GGCTGGGACGAGCAGTGAAGACCATCTCTG  -69

WT   ATCAACCCCAGGCCCACGATAATGACCTCATGCTGCTGAAGCT...CCAGTCCCATTGGTAAGGAGCCCTGGGCCTGAAAGTACAAA
24B  ATCAACCCCAGGCCCACGATAATGACCTCATGCTGCTGAAG--...--TACAAAGCTGAAAGTACAAAGCTGGCCTGAAAGTACAAA  -108, +23
20C  ATCAACCCCAGGCCCACGATAATGACCTCATGCTGCTGAAG--...--TACAAAGCTGAAAGTACAAAGCTGGCCTGAAAGTACAAA  -108, +23
```

Figure 17. Genotyping of F0 (founder) mice. The 34 founder mice born to CD-1 foster mothers were screened for mutations in the TALEN target site in exon 3 of *Klk14* (**B**) by PCR from genomic DNA obtained from tail biopsies and subsequent PstI digest (**A**) and the presence of mutations was further confirmed by sequencing (**D**). From the 34 founders examined, 16 mice (46 %) were found to have mutations in the TALEN target site (**C**). Sequencing revealed mosaicism in 4 of the founder mice (**C**, **D**).

The F1 generation obtained from selected founder mice was genotyped for mutations in *Klk14* transmitted from the founder parent and two candidate mutations were selected to establish the Klk5$^{-/-}$Klk14^{del69} and Klk5$^{-/-}$Klk14^{del5} strains. Heterozygous F1 generation Klk5$^{+/-}$Klk14$^{+/-}$ mice carrying the desired Klk14^{del69} and Klk14^{del5} alleles were bred to the C57Bl/6NCrl background to minimize the risk of mutations resulting from off-target activity of the TALE nucleases being carried over into the derived strains.

Heterozygous F2 generation Klk5$^{+/-}$Klk14$^{+/-}$ mice born to different parents were subsequently crossed, resulting in F3 generation offspring that included Klk5$^{-/-}$Klk14$^{-/-}$ double-deficient individuals in both Klk5$^{-/-}$Klk14^{del69} and Klk5$^{-/-}$Klk14^{del5} strains.

All F2 and the majority of F3 litters were genotyped for Klk5$^{tm2a(KOMP)Wtsi}$ (Klk5$^{-/-}$) using PCR (Fig. 18) additionally to *Klk14* genotyping (RYDER *et al.* 2013). It was found that the *Klk14* genotype corresponded to the *Klk5* genotype in all individuals analyzed (data not shown).

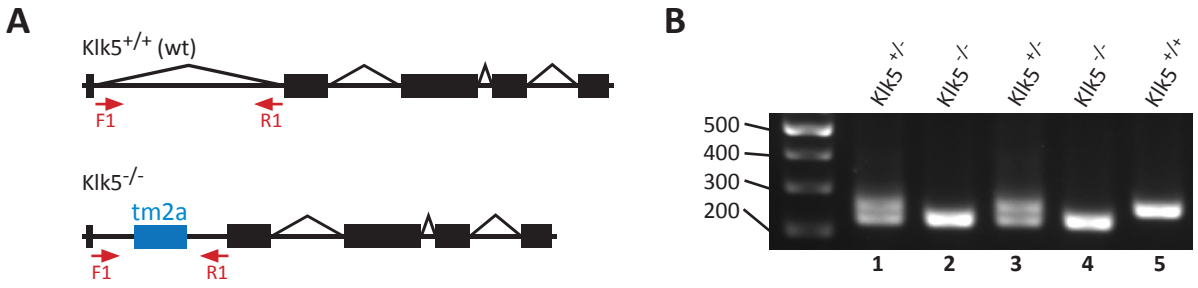

Figure 18. Genotyping for Klk5$^{tm2a(KOMP)Wtsi}$ (Klk5$^{-/-}$). The presence of the tm2a cassette between exon 1 and exon 2 of *Klk5* in the Klk5$^{tm2a(KOMP)Wtsi}$ (Klk5$^{-/-}$) allele (**A**) leads to a shorter PCR product compared to wild type (**B**).

6.4.1 The Klk5$^{-/-}$Klk14^{del69} Strain

The Klk5$^{-/-}$Klk14^{del69} strain was derived from founder 24. The mosaic founder 24 was bred with Klk5$^{tm2a(KOMP)Wtsi}$ (Klk5$^{-/-}$) mates to obtain the F1 generation. From the two different mutations identified in founder 24 (Fig. 17 D) only the 69 bp deletion (Klk14^{del69} allele) was transmitted to offspring in 1:1 ratio (Fig. 19 D) to wild type. The deletion within the exon 3 *Klk14* TALEN target site in the Klk5$^{-/-}$Klk14^{del69} strain led to the absence of the PstI site within the targeted locus, therefore the resulting offspring could be genotyped for *Klk14* using RFLP analysis via PstI cleavage (Fig. 19 B). The 69 bp deletion however was extensive enough to be visible as a truncated PCR product (Fig. 19 A), thus making PstI digest unnecessary for identification of the Klk14^{del69} allele. The PCR products of all F1 mice were sequenced to confirm uniform transmission of the Klk14^{del69} allele (Fig. 19 C).

The 69 bp deletion within exon 3 of *Klk14* was expected to lead to truncated KLK14, missing 23 amino acids in positions from 108 to 130. Importantly, among the deleted amino acids in the Klk5$^{-/-}$Klk14^{del69} strain is Asp110. Asp110, along with His66 and Ser203 form the catalytic triad typical for serine endopeptidases and necessary for their function (PAVLOPOPULOU *et al.* 2010, Fig. 19 E).

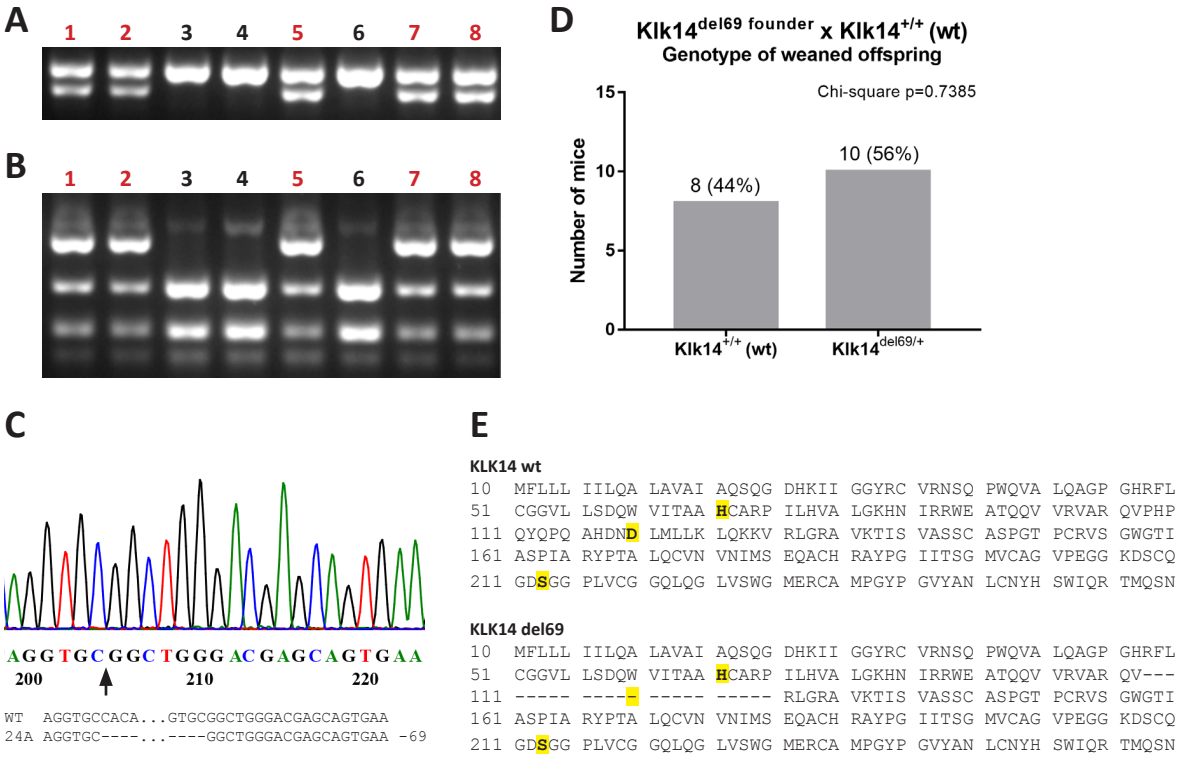

Figure 19. Analysis of the Klk5$^{-/-}$Klk14^{del69} strain. Founder 24 was bred with Klk5$^{tm2a(KOMP)Wtsi}$ (Klk5$^{-/-}$) mates to obtain the F1 generation. The F1 mice were analyzed by PCR and RFLP (**A**, **B**) and the Klk14^{del69} allele was confirmed by Sanger sequencing (**C**). Transmission of the Klk14^{del69} allele from the founder conformed to the predicted 1:1 Mendelian ratio (**D**). The 69 bp deletion was expected to result in the absence of 23 amino acids in KLK14, including D. Amino acids of the catalytic triad are highlighted in yellow (**E**).

6.4.2 The Klk5$^{-/-}$Klk14^{del5} Strain

The Klk5$^{-/-}$Klk14^{del5} strain was derived from founder 30. In this case, founder 30 was bred with C57Bl/6NCrl mates to obtain the F1 generation. Interestingly, out of 28 F1 mice obtained, only 3 were identified to carry the 5 bp deletion (Klk14^{del5} allele). This result deviates from the expected Mendelian ratio of 1:1 sufficiently to be statistically significant, implying that founder 30 was a mosaic with only a fraction of germ line cells carrying the Klk14^{del5} allele. The 5 bp deletion within exon 3 of *Klk14* resulted in the absence of the PstI site within the targeted locus similar to the Klk14^{del69} allele described in the previous chapter, therefore genotyping for *Klk14* could be performed via RFLP analysis with PstI digest of the TALEN target site PCR product (Fig. 20 A). One male (Fig. 20 A, in red) and two females were found to carry the Klk14^{del5} allele in the F1 generation. The genotype of all F1 heterozygous Klk5$^{+/-}$Klk14$^{del5/+}$ mice was confirmed by Sanger sequencing of the TALEN target site (Fig. 20 B). Only the heterozygous Klk5$^{+/-}$Klk14$^{del5/+}$ male was chosen for breeding. Due to contamination of the sample with the wild type allele, sequencing was repeated and the presence of the Klk14^{del5} allele was confirmed (data not shown).

The 5 bp deletion within exon 3 of *Klk14* was expected to lead to frameshift following Lys125. This mutation was expected to result in a truncated KLK14 in the Klk5$^{-/-}$Klk14^{del5} strain, lacking the Ser203 form the catalytic triad and a premature stop-codon (Fig. 20 D) compared to wild type KLK14 (Fig. 19 E).

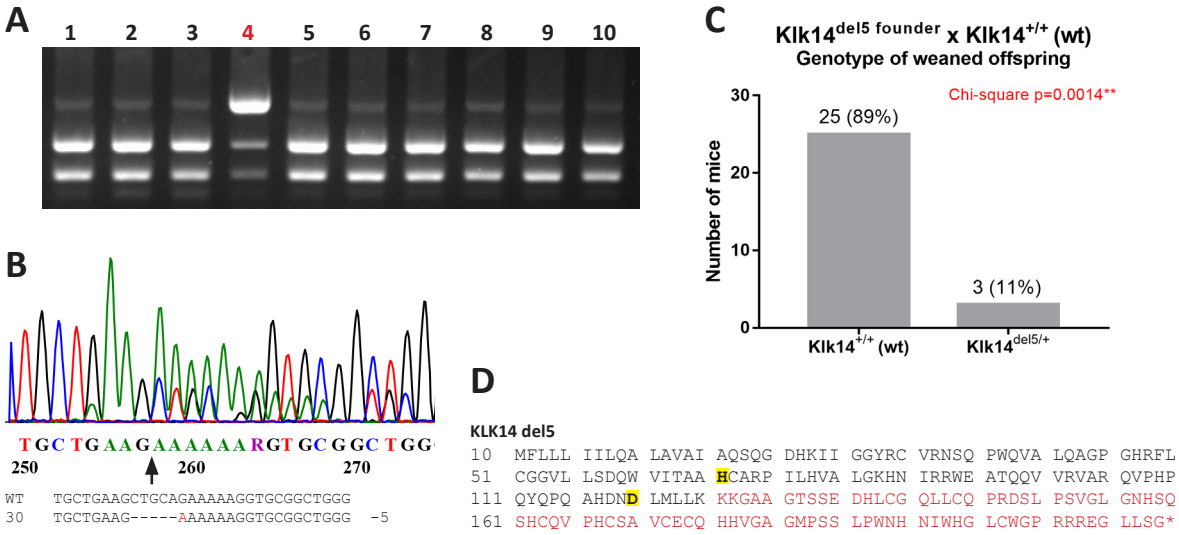

Figure 20. Analysis of the Klk5$^{-/-}$Klk14^{del65} strain. Founder 30 was bred with C57Bl/6NCrl mates to obtain the F1 generation. The F1 mice were analyzed by RFLP using PstI digest (**A**) and the Klk14^{del5} allele was confirmed with Sanger sequencing (**B**). Transmission of the Klk14^{del5} allele from the founder did not conform to the predicted 1:1 Mendelian ratio, implying germ line mosaicism in the founder (**C**). The 5 bp deletion was expected to lead to frameshift following amino acid 125 and resulting in a premature stop codon. Amino acids of the catalytic triad are highlighted in yellow (**D**).

6.5. RNA Isolation and *Klk14* cDNA Analysis in Double-deficient Klk5$^{-/-}$Klk14$^{del69/+}$ and Klk5$^{-/-}$Klk14$^{del5/+}$ Mice

In order to confirm that both double-deficient Klk5$^{-/-}$Klk14$^{del69/del69}$ and Klk5$^{-/-}$Klk14$^{del5/del5}$ mice do not produce mRNA transcripts that would allow the synthesis of functional KLK14, mRNA was isolated and analysed in respect to the presence of *Klk14* transcripts. The quality of purified RNA was verified by gel electrophoresis, where 18S and 23S rRNA bands could be clearly distinguished indicating that the isolated RNA was isolated successfully without degrading (Fig. 21 A). Following in vitro reverse transcription, *Klk14* cDNA was amplified by PCR using primers annealing to exon 3 and exon 4 (Fig. 21 B). The amplified cDNA locus was expected to contain the indel mutations in both Klk5$^{-/-}$Klk14^{del69} and Klk5$^{-/-}$Klk14^{del5} strains. *Klk14* cDNA was found to be present in equal amounts in all samples analyzed (Fig. 21 B), with the truncation caused by the 69 bp deletion clearly present in both double-deficient Klk5$^{-/-}$Klk14$^{del69/del69}$ P8 pups. The PCR products were further analyzed by Sanger sequencing. The boundary between exon 3 and exon 4 was clearly present in all samples, indicating no contamination of the cDNA with genomic DNA (Fig. 21 C). The *Klk14* cDNA of both double-deficient Klk5$^{-/-}$Klk14$^{del69/del69}$ and Klk5$^{-/-}$Klk14$^{del5/del5}$ P8 pups was found to contain the indel mutations present in the *Klk14* gene (Fig. 21 D, E).

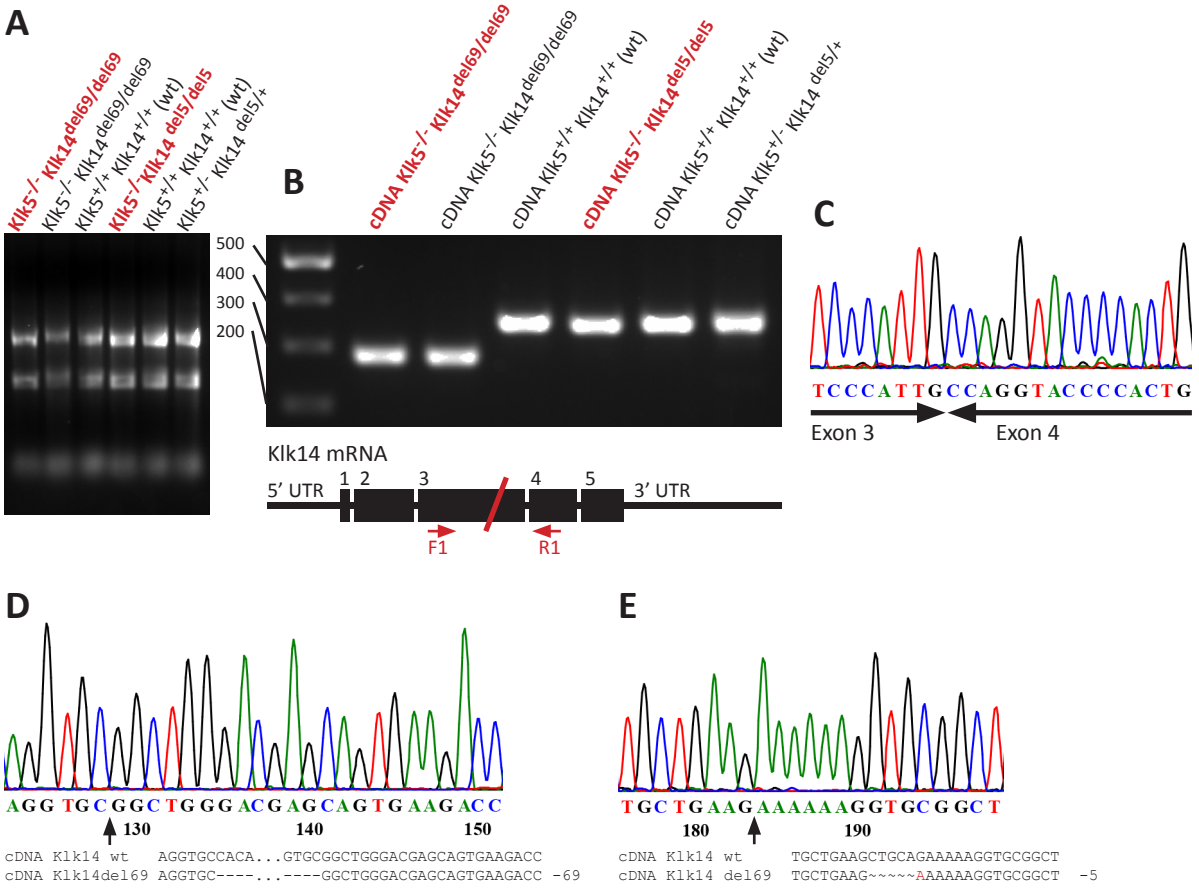

Figure 21. Analysis of *Klk14* cDNA prepared from RNA isolated from dorsal skin of double-deficient Klk5$^{-/-}$Klk14$^{del69/del69}$ and Klk5$^{-/-}$Klk14$^{del5/del5}$ P8 pups. The quality of isolated and purified RNA was assessed by gel electrophoresis, where 18S and 23S rRNA bands can be clearly distinguished (**A**). cDNA was prepared by in vitro reverse transcription and *Klk14* mRNA was amplified using primers (F1, R1) annealing to exon 3 and exon 4 (**B**). The resulting PCR products were sequenced. The boundary between exon 3 and exon 4 was present in the sequences obtained, indicating *Klk14* cDNA as template (**C**). Double-deficient Klk5$^{-/-}$Klk14$^{del69/del69}$ and Klk5-/-Klk14$^{del5/del5}$ P8 pups were shown to express mRNA with their respective mutations present (**D**, **E**).

6.6. Preliminary Phenotype Analysis in Double-deficient Klk5$^{-/-}$Klk14$^{del69/+}$ and Klk5$^{-/-}$Klk14$^{del5/+}$ Mice

Heterozygous Klk5$^{+/-}$Klk14$^{del69/+}$ and Klk5$^{+/-}$Klk14$^{del5/+}$ F2 generation mice born to different parents were used to form Klk5$^{+/-}$Klk14$^{del69/+}$ x Klk5$^{+/-}$Klk14$^{del69/+}$ and Klk5$^{+/-}$Klk14$^{del5/+}$ x Klk5$^{+/-}$Klk14$^{del5/+}$ (het x het) breeding pairs. The resulting F3 generation offspring (expected to contain Klk5$^{-/-}$Klk14$^{-/-}$ double-deficient along with wild type and heterozygous individuals) was analyzed with respect to viability, genotype and sex distribution, and presence of abnormal epidermal phenotype.

From the het x het breedings, up to 80 F3 generation mice in both Klk5$^{-/-}$Klk14^{del69} and Klk5$^{-/-}$Klk14^{del5} strains were weaned. No deviation from the expected 1:1 male to female ratio was observed in either of the strains (Fig. 22 A). Similarly, the genotype distribution conformed to the

expected 1:2:1 Mendelian distribution in both of the strains, indicating that the Klk5$^{-/-}$Klk14$^{-/-}$ double-deficient phenotype had no significant impact on viability and survival of the mice until weaning age. (Fig. 22 B). The adult mice continued to develop normally, displaying no observable anomalies compared to their heterozygous and wild type littermates (data not shown).

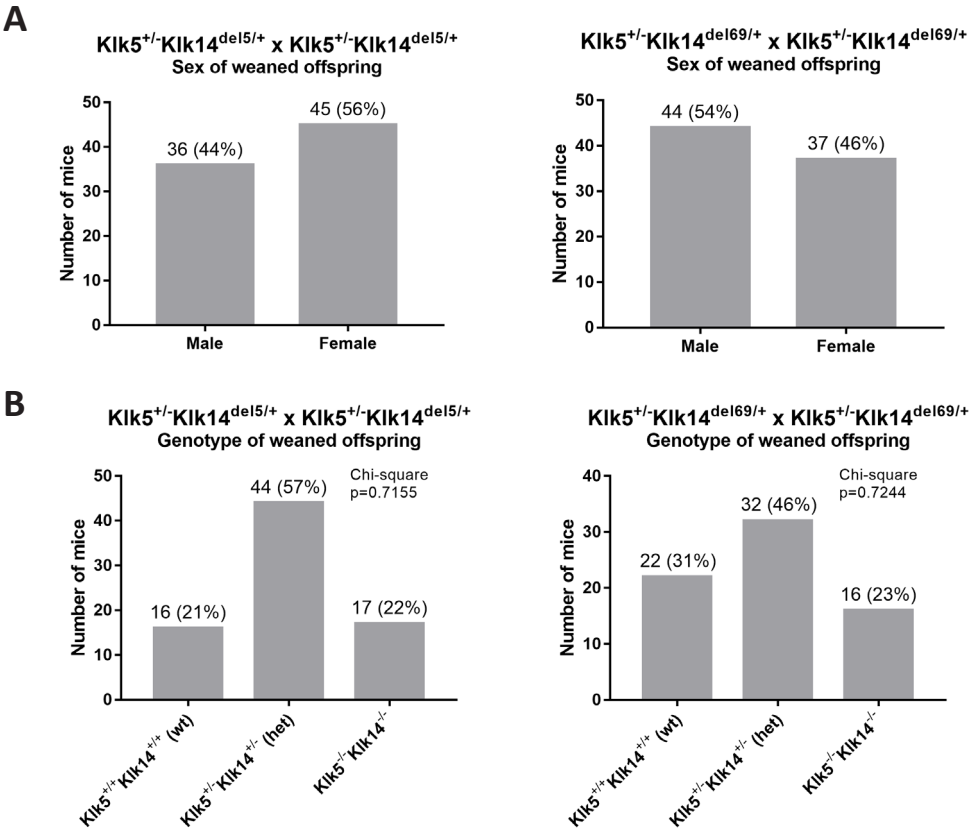

Figure 22. Sex and genotype distribution in weaned offspring (F3 generation) from Klk5$^{+/-}$Klk14$^{del5/+}$ x Klk5$^{+/-}$Klk14$^{del5/+}$ and Klk5$^{+/-}$Klk14$^{del69/+}$ x Klk5$^{+/-}$Klk14$^{del69/+}$ breedings. Sex distribution in the F3 generation of both strains conformed to the expected 1:1 ratio (**A**). The distribution of the Klk14^{del69} and Klk14^{del5} alleles among the F3 generation also conformed to the predicted 1:2:1 Mendelian ratio (**B**).

No differences between the Klk5$^{-/-}$Klk14^{del69} and Klk5$^{-/-}$Klk14^{del5} strains were observed. For skin and hair morphology analysis, postnatal day 8 (P8) pups of both strains were selected (data shown from Klk5$^{-/-}$Klk14^{del69} strain pups only). The P8 pups did not display any gross morphological differences from their heterozygous and wild type littermates (Fig. 23 A, B). The weight of P8 pups showed a relatively high variability both within individual litters and overall, but there was no apparent correlation of weight and genotype of the pups (Fig. 23 C).

Upon closer examination, slight scaling that was most pronounced on abdominal skin could be consistently observed in P8 double-deficient Klk5$^{-/-}$Klk14$^{del69/del69}$ and Klk5$^{-/-}$Klk14$^{del5/del5}$ pups when compared to their heterozygous or wild type littermates (Fig. 24 A). In order to undertake a more detailed analysis of the epidermis, whole-body paraffin-embedding, sectioning and

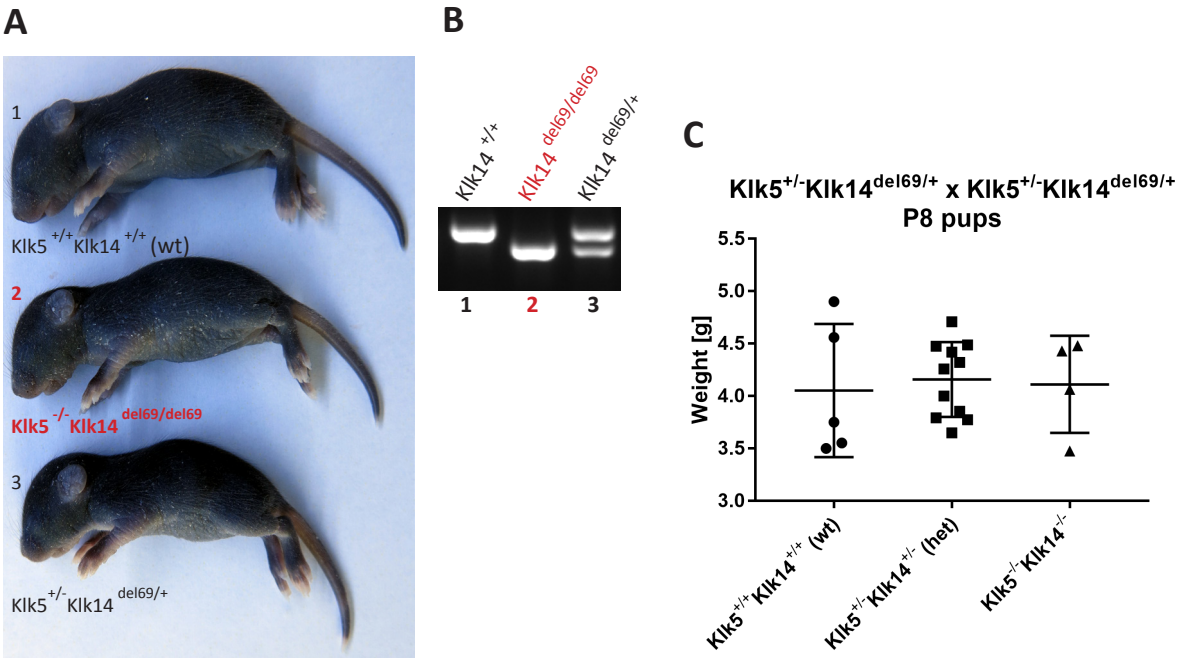

Figure 23. Gross morphology and weight distribution in postnatal day 8 (P8) pups (F3 generation) from Klk5$^{+/-}$Klk14$^{del69/+}$ x Klk5$^{+/-}$Klk14$^{del69/+}$ breedings. Double-deficient Klk5$^{-/-}$Klk14$^{del69/del69}$ P8 pups (**A** 2, **B** 2) show no readily apparent phenotypic change compared to their wild type Klk5$^{+/+}$Klk14$^{+/+}$ (**A** 1, **B** 1) and heterozygous Klk5$^{+/-}$Klk14$^{del69/+}$ (**A** 3, **B** 3) littermates. Weight of P8 pups does not correlate with genotype (**C**).

hematoxylin/eosin staining of P8 pups was performed. Histological examination of both dorsal and ventral epidermis did however not reveal any significant differences between double-deficient P8 Klk5$^{-/-}$Klk14$^{del69/del69}$ pups when compared to their heterozygous or wild type littermates (Fig. 24 C, D, E). No abnormalities in hair shaft morphology and *stratum corneum* thickness could be determined. The epidermal layers were properly differentiated, *vibrissae* were intact and fur was developing normally.

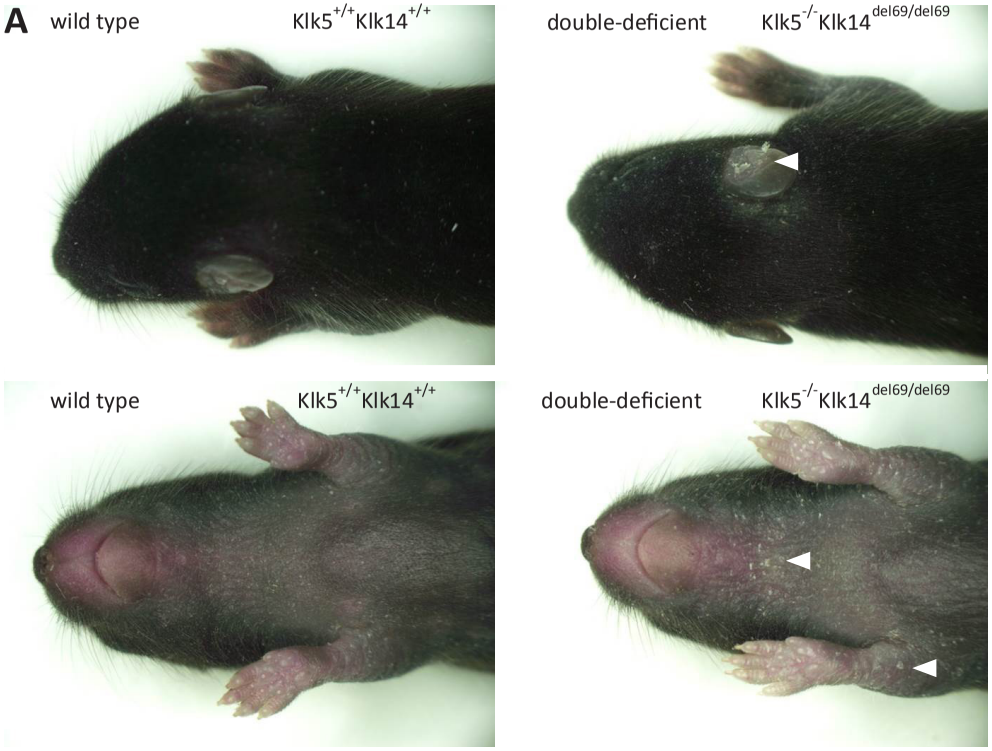
A
wild type
Klk5+/+Klk14+/+
double-deficient
Klk5-/-Klk14del69/del69
wild type
Klk5+/+Klk14+/+
double-deficient
Klk5-/-Klk14del69/del69

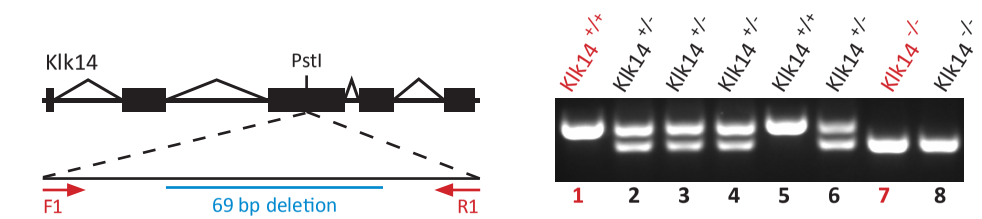
B
Klk14
PstI
F1
69 bp deletion
R1

Klk14 +/+
Klk14 +/-
Klk14 +/-
Klk14 +/-
Klk14 +/+
Klk14 +/-
Klk14 -/-
Klk14 -/-
1
2
3
4
5
6
7
8

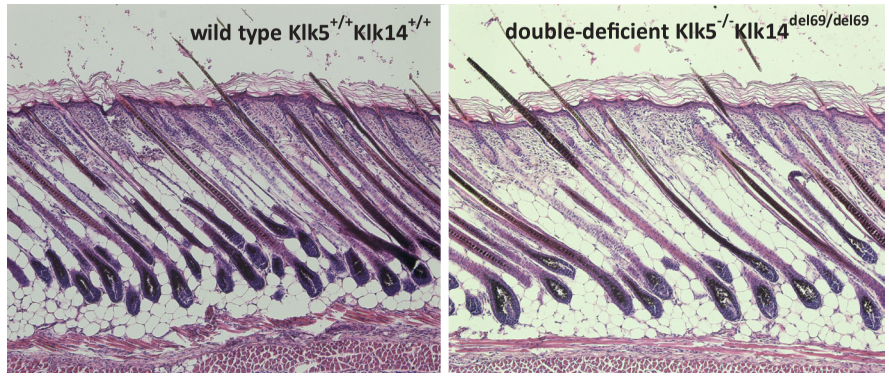
C
wild type Klk5+/+Klk14+/+
double-deficient Klk5-/-Klk14del69/del69

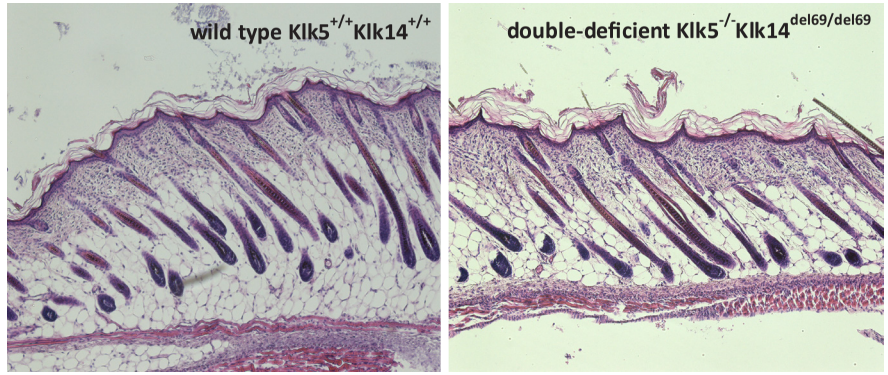
D
wild type Klk5+/+Klk14+/+
double-deficient Klk5-/-Klk14del69/del69

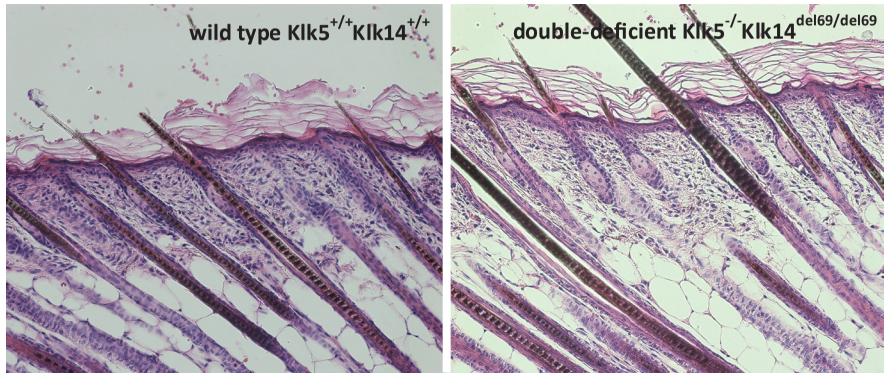
E
wild type Klk5+/+Klk14+/+
double-deficient Klk5-/-Klk14del69/del69

Figure 24 (previous page). Detailed analysis of epidermal and hair morphology of Klk5$^{-/-}$Klk14^{del69} strain postnatal day 8 (P8) pups. The comparison of P8 wild type Klk5$^{+/+}$Klk14$^{+/+}$ and double-deficient Klk5$^{-/-}$Klk14$^{del69/del69}$ littermates (**B** 1 and 7, in red) revealed no abnormalities of fur and *vibrissae* (**A**). Slight epidermal scaling was present in double-deficient Klk5$^{-/-}$Klk14$^{del69/del69}$ pups, being most pronounced on ventral epidermis (**A**, white arrows). Histology of dorsal (**C**, **E**) and ventral (**D**) epidermis shows no difference in hair shaft morphology and no differences in *stratum corneum* thickness, nor in overall epidermal morphology (**C**, **D**, **E**).

7. Discussion

7.1. TALEN and CRISPR/Cas9 Systems Show Comparable Efficiency in Surrogate Reporter-based *In Vitro* Assay

Recently, the CRISPR/Cas9 technology has emerged as the programmable nuclease (PN) technology for genome editing preferred by the scientific community. A strong argument in favor of CRISPR/Cas9 over TALENs is the relative ease of preparation. Indeed, preparation of pX330 vectors targeting exon 2 of *Klk14* was far less time-consuming and more efficient than the preparation of TALEN pairs targeting exon 2 and exon 3 of the same gene (chapter 6.1., Fig. 10, 12), while both systems showed comparable activity in cell culture, with the TALENs displaying marginally higher activity (chapter 6.2., Fig. 16). However, another factor that merits consideration when comparing the two PN systems is the likelihood of off-target cleavage. Here, the advantage of TALENs is the requirement of both pairs successfully binding their target DNA to form an active FokI nuclease domain, whereas Cas9 is an active nuclease not dependent on dimerization. In fact, several attempts at reducing the frequency of off-target cleavage in the CRISPR/Cas9 system have been undertaken, notably the conversion of Cas9 to function as a nickase or employment of Cas9 with deactivated nuclease activity but fused instead to the dimerization-requiring FokI nuclease domain (TERAO *et al.* 2016). Both approaches require a Cas9 pair to bind their target DNA, similar to the TALEN target DNA recognition and cleavage mechanism. However, diminished cleavage efficiency of modified Cas9 as compared to native Cas9 nuclease could be an issue. Consequently, we decided to employ the TALENs over the CRISPR/Cas9 system for targeting *Klk14*.

Additionally, it is important to note that the activity of all PNs that were tested in cell culture reflected as the presence of RFP fluorescence is not a direct indicator of genomic DNA cleavage efficiency. Epigenetic factors such as methylation and chromatin structure of the targeted genomic DNA locus could influence the ability of PN binding and therefore cleavage efficiency, as opposed to binding to the pARv-RFP reporter vector DNA (VALTON *et al.* 2014). To this effect, we performed additional analysis of genomic DNA in the targeted cells by enriching for GFP and RFP positive cells via FACS and subsequent sequencing of the *Klk14* locus (data not shown).

7.2. Founder Mice Obtained from TALEN Microinjection into Zygotes Contain Mutations in the Targeted *Klk14* Locus

From 34 mice born in the founder generation, 16 mice (46 %) have been shown to carry mutated *Klk14* alleles (chapter 6.3., Fig. 17). TALEN cleavage efficiency in microinjected zygotes therefore was considerably high. Interestingly, a specific mutation, a 108 bp deletion combined with a 23 bp insertion, was discovered to have occurred independently in two of the founder mice. Additionally, the same mutation within the targeted *Klk14* locus was detected in genomic DNA analysis of the TALEN-targeted cells (data not shown). The insertion consists of repeats of a short sequence adjacent to the target site. Repair of the DSB induced by TALEN cleavage could have occurred in both founders independently via the microhomology-mediated end-joining (MMEJ)

pathway rather than the non-homologous end-joining (NHEJ) pathway and thus have led to the same mutation present in both mice and in the cell line (KENT *et al.* 2015). Notably, the 69 bp deletion present in the Klk14^{del69} allele is also framed by 5 bp long GGTGC sequences, implying that in this case, MMEJ might have occurred as well.

Lastly, there was a relatively high prevalence of mosaicism for the targeted *Klk14* locus observed in the founder mice. Out of the 12 founders identified to carry mutations in *Klk14*, 4 (25 %) were found to carry more than one type of mutation based on tail biopsy analysis. Additionally, one more founder was identified as a putative mosaic by statistical analysis of genotype ratio in the offspring (chapter 6.4.2, Fig. 20 C). Due to this observation, it is conceivable that the rate of mosaicism could be even higher than the rate identified from tail biopsies alone. Mosaicism in mice generated by injection of PN mRNA into cytoplasm and pronuclei of zygotes is a known phenomenon (YEN *et al.* 2014, OLIVER *et al.* 2015). The occurrence of this type of mosaicism is being attributed to the activity of the microinjected PNs extending past the early divisions of the one cell stage zygote (LI *et al.* 2014).

7.3. *Klk14* mRNA Expressed in Both KLK5 and KLK14 Double-deficient Strains Does Not Allow Synthesis of Functional KLK14

Both of the mutations present in the established Klk5$^{-/-}$Klk14^{del5} and Klk5$^{-/-}$Klk14^{del69} strains are expected to lead to the expression of proteolytically inactive KLK14. In both cases, the catalytic triad necessary for serine protease function is disrupted (chapter 6.4., Fig. 19 and Fig. 20). Furthermore, in the Klk5$^{-/-}$Klk14^{del5} strain, a frameshift and subsequent premature stop codon should lead to expression of a truncated KLK14. Consequently, the Klk5$^{-/-}$Klk14^{del5} strain was selected for future experiments and in-depth analysis of phenotype. Analysis of mRNA expressed in double-deficient mice in both strains further confirmed the presence of *Klk14* mRNA transcripts that do not allow the synthesis of functional KLK14 (chapter 6.5, Fig. 21). Based on these findings, it is safe to assume both strains are indeed KLK5 and KLK14 double-deficient. However, definitive confirmation warrants analysis of KLK14 on the protein level.

Initially, the protein fraction that was obtained from the skin samples of double-deficient mice along with the mRNA could be analyzed via western blot and an antibody specific for murine KLK14 or alternatively identification by mass spectrometry (KARAKOSTA *et al.* 2016). However, a more conclusive analysis that focuses on the catalytic activity rather than simple presence of the enzyme would be casein zymography of the epidermal extract (BRATTSAND *et al.* 2005).

7.4. Both KLK5 and KLK14 Double-deficient Strains Show No Obvious Cutaneous Phenotype

Preliminary analysis of phenotype in both Klk5$^{-/-}$Klk14^{del5} and Klk5$^{-/-}$Klk14^{del69} strains has not revealed any significant differences between double-deficient Klk5$^{-/-}$Klk14$^{del69/del69}$ and Klk5$^{-/-}$Klk14$^{del5/del5}$ mice and their heterozygous or wild type littermates (chapter 6.6.). This result

is in line with our previously stated hypothesis that epidermal KLKs are at least to some degree redundant in their respective functions rather than forming a hierarchical proteolytic cascade (chapter 4.4.2.). In the context of the phenotype we observed in KLK5 and KLK7 double-deficient mice, we can conclude that it is likely that KLK7 (along with other epidermal proteases) is sufficient to ensure proper keratinocyte differentiation and corneocyte desquamation even in the absence of both KLK5 and KLK14, while KLK14 is not capable of the same in the absence of KLK5 and KLK7.

The slight increase in epidermal scaling observed predominantly on ventral skin of postnatal day 8 (P8) $Klk5^{-/-}Klk14^{del69/del69}$ and $Klk5^{-/-}Klk14^{del5/del5}$ pups is not due to double-deficiency for both KLK5 and KLK14, since we observed a similar phenotype in P8 $Klk5^{-/-}$ pups (Supplementary fig. 1), indicating that the scaling can be explained by KLK5 deficiency alone. Indeed, KLK14 deficient mice do not display an increase in scaling when compared to their wild type littermates (Supplementary fig. 2).

Once the absence of functional KLK14 is confirmed on the protein level, a much more rigorous analysis of phenotype in the KLK5 and KLK14 double-deficient strains should follow. One possible direction of research would be various challenges, such as wound healing and induced dermatitis assays, particularly in the context of the ability of both KLK5 and KLK14 to activate the pro-inflammatory PAR2 receptor that is co-expressed with both KLKs in the epidermis. Indeed, we have already performed an induced dermatitis experiment by croton oil application and subsequent ear thickness measurement on KLK14 deficient mice (Supplementary fig. 3), indicating no difference in the increase of ear thickness between knock-out and wild type animals. In the absence of both KLK14 and KLK5 however, the resulting decrease in PAR2-mediated pro-inflammatory signalling could have an impact.

Finally, we are already breeding the $Klk5^{-/-}Klk14^{del5}$ strain to our LEKTI deficient strain. We expect that the resultant KLK5, KLK14 and LEKTI triple-deficient mice could provide important insight into the role of KLK14 in the pathology of Netherton syndrome.

8. Summary

Both transcription activator-like effector nucleases (TALENs) and guide RNA (gRNA) for CRISPR/Cas9 were designed to target exons 2 and 3 of the murine *Klk14* gene. Vectors expressing the designed programmable nucleases (PNs) were prepared and their activity was compared in cell culture, using the surrogate reporter vector pARv-RFP and RFP expression reconstitution. For the selected TALEN pair targeting exon 3 of *Klk14*, mRNA was prepared by *in vitro* transcription and polyadenylation that was subsequently used to microinject KLK5-deficient zygotes. The resulting founder generation was analyzed in respect to mutations in the targeted *Klk14* exon 3 locus. Founders carrying a 65 bp deletion and a 5 bp deletion in this locus were bred to C57Bl/6NCrl background and two putative KLK5 and KLK14 double-deficient mouse strains were established, $Klk5^{-/-}Klk14^{del69}$ and $Klk5^{-/-}Klk14^{del5}$. It was confirmed that both double-deficient $Klk5^{-/-}Klk14^{del69/del69}$ and $Klk5^{-/-}Klk14^{del5/del5}$ mice do not produce mRNA transcripts allowing synthesis of functional KLK14 by isolating and analyzing mRNA obtained from dorsal skin samples. Finally, the phenotype of offspring from $Klk5^{+/-}Klk14^{del69/+}$ x $Klk5^{+/-}Klk14^{del69/+}$ and $Klk5^{+/-}Klk14^{del5/+}$ x $Klk5^{+/-}Klk14^{del5/+}$ (het x het) breedings was analyzed. No difference between wild type and knock-out animals with respect to viability, genotype and sex distribution and presence of abnormal epidermal phenotype was observed.

9. Literature

Bhogal, R. K., P. E. Mouser, et al. (2014). "Protease activity, localization and inhibition in the human hair follicle." Int J Cosmet Sci 36(1): 46-53.

Bitoun, E., S. Chavanas, et al. (2002). "Netherton syndrome: disease expression and spectrum of SPINK5 mutations in 21 families." J Invest Dermatol 118(2): 352-361.

Brattsand, M., K. Stefansson, et al. (2005). "A proteolytic cascade of kallikreins in the stratum corneum." J Invest Dermatol 124(1): 198-203.

Briot, A., C. Deraison, et al. (2009). "Kallikrein 5 induces atopic dermatitis-like lesions through PAR2-mediated thymic stromal lymphopoietin expression in Netherton syndrome." J Exp Med 206(5): 1135-1147.

Candi, E., R. Schmidt, et al. (2005). "The cornified envelope: a model of cell death in the skin." Nat Rev Mol Cell Biol 6(4): 328-340.

Caubet, C., N. Jonca, et al. (2004). "Degradation of corneodesmosome proteins by two serine proteases of the kallikrein family, SCTE/KLK5/hK5 and SCCE/KLK7/hK7." J Invest Dermatol 122(5): 1235-1244.

Cermak, T., E. L. Doyle, et al. (2011). "Efficient design and assembly of custom TALEN and other TAL effector-based constructs for DNA targeting." Nucleic Acids Res 39(12): e82.

Chavanas, S., C. Bodemer, et al. (2000). "Mutations in SPINK5, encoding a serine protease inhibitor, cause Netherton syndrome." Nat Genet 25(2): 141-142.

Cong, L., F. A. Ran, et al. (2013). "Multiplex genome engineering using CRISPR/Cas systems." Science 339(6121): 819-823.

Deraison, C., C. Bonnart, et al. (2007). "LEKTI fragments specifically inhibit KLK5, KLK7, and KLK14 and control desquamation through a pH-dependent interaction." Mol Biol Cell 18(9): 3607-3619.

Descargues, P., C. Deraison, et al. (2005). "Spink5-deficient mice mimic Netherton syndrome through degradation of desmoglein 1 by epidermal protease hyperactivity." Nat Genet 37(1): 56-65.

Dow, L. E. and S. W. Lowe (2012). "Life in the fast lane: mammalian disease models in the genomics era." Cell 148(6): 1099-1109.

Doyle, E. L., N. J. Booher, et al. (2012). "TAL Effector-Nucleotide Targeter (TALE-NT) 2.0: tools for TAL effector design and target prediction." Nucleic Acids Res 40(Web Server issue): W117-122.

Drucker, K. L., C. Gianinni, et al. (2015). "Prognostic significance of multiple kallikreins in high-grade astrocytoma." BMC Cancer 15: 565.

Elias, P. M. and M. Schmuth (2009). "Abnormal skin barrier in the etiopathogenesis of atopic dermatitis." Curr Opin Allergy Clin Immunol 9(5): 437-446.

Emami, N., D. Deperthes, et al. (2008). "Major role of human KLK14 in seminal clot liquefaction." J Biol Chem 283(28): 19561-19569.

Flemr, M., R. Malik, et al. (2013). "A retrotransposon-driven dicer isoform directs endogenous small interfering RNA production in mouse oocytes." Cell 155(4): 807-816.

Flicek, P., M. R. Amode, et al. (2014). "Ensembl 2014." Nucleic Acids Res 42(Database issue): D749-755.

Fortugno, P., A. Bresciani, et al. (2011). "Proteolytic activation cascade of the Netherton syndrome-defective protein, LEKTI, in the epidermis: implications for skin homeostasis." J Invest Dermatol 131(11): 2223-2232.

Furio, L., G. Pampalakis, et al. (2015). "KLK5 Inactivation Reverses Cutaneous Hallmarks of Netherton Syndrome." PLoS Genet 11(9): e1005389.

Gaj, T., C. A. Gersbach, et al. (2013). "ZFN, TALEN, and CRISPR/Cas-based methods for genome engineering." Trends Biotechnol 31(7): 397-405.

Haneckova, R. (2014). "Genome editing using programmable endonucleases." Bachelor thesis, Charles University in Prague, Prague.

Haneckova, R. (2016). "The pAR reporter system for efficient selection of TALEN/CRISPR targeted cells." 9th Institute of Molecular Genetics PhD Conference, Czech Republic, Prague, 3. 6. 2016.

Hewett, D. R., A. L. Simons, et al. (2005). "Lethal, neonatal ichthyosis with increased proteolytic processing of filaggrin in a mouse model of Netherton syndrome." Hum Mol Genet 14(2): 335-346.

Hovnanian, A. (2013). "Netherton syndrome: skin inflammation and allergy by loss of protease inhibition." Cell Tissue Res 351(2): 289-300.

Karakosta, T. D., A. Soosaipillai, et al. (2016). "Quantification of Human Kallikrein-Related Peptidases in Biological Fluids by Multi-Platform Targeted Mass Spectrometry Assays." Mol Cell Proteomics.

Kent, T., G. Chandramouly, et al. (2015). "Mechanism of microhomology-mediated end-joining promoted by human DNA polymerase theta." Nat Struct Mol Biol 22(3): 230-237.

Kim, Y. H., S. Ramakrishna, et al. (2014). “Enrichment of cells with TALEN-induced mutations using surrogate reporters.” Methods 69(1): 108-117.

Komatsu, N., M. Takata, et al. (2003). “Expression and localization of tissue kallikrein mRNAs in human epidermis and appendages.” J Invest Dermatol 121(3): 542-549.

Li, C., R. Qi, et al. (2014). “Simultaneous gene editing by injection of mRNAs encoding transcription activator-like effector nucleases into mouse zygotes.” Mol Cell Biol 34(9): 1649-1658.

Lieber, M. R. (2010). “The mechanism of double-strand DNA break repair by the nonhomologous DNA end-joining pathway.” Annu Rev Biochem 79: 181-211.

List, K., C. C. Haudenschild, et al. (2002). “Matriptase/MT-SP1 is required for postnatal survival, epidermal barrier function, hair follicle development, and thymic homeostasis.” Oncogene 21(23): 3765-3779.

Lundwall, Å. (2013). “Old genes and new genes: the evolution of the kallikrein locus.” Thromb Haemost 110(3): 469-475.

Mali, P., L. Yang, et al. (2013). “RNA-guided human genome engineering via Cas9.” Science 339(6121): 823-826.

McGrath, J. A. and J. Uitto (2008). “The filaggrin story: novel insights into skin-barrier function and disease.” Trends Mol Med 14(1): 20-27.

Menon, G. K., P. M. Elias, et al. (1992). “Localization of calcium in murine epidermis following disruption and repair of the permeability barrier.” Cell Tissue Res 270(3): 503-512.

Miyai, M., Y. Matsumoto, et al. (2014). “Keratinocyte-specific mesotrypsin contributes to the desquamation process via kallikrein activation and LEKTI degradation.” J Invest Dermatol 134(6): 1665-1674.

Molin, S., J. Merl, et al. (2015). “The hand eczema proteome: imbalance of epidermal barrier proteins.” Br J Dermatol 172(4): 994-1001.

Mortz, C. G., K. E. Andersen, et al. (2015). “Atopic dermatitis from adolescence to adulthood in the TOACS cohort: prevalence, persistence and comorbidities.” Allergy 70(7): 836-845.

Ohman, H. and A. Vahlquist (1994). “In vivo studies concerning a pH gradient in human stratum corneum and upper epidermis.” Acta Derm Venereol 74(5): 375-379.

Oliver, D., S. Yuan, et al. (2015). “Pervasive Genotypic Mosaicism in Founder Mice Derived from Genome Editing through Pronuclear Injection.” PLoS One 10(6): e0129457.

Olsson, A. Y. and A. Lundwall (2002). “Organization and evolution of the glandular kallikrein locus in Mus musculus.” Biochem Biophys Res Commun 299(2): 305-311.

Ovaere, P., S. Lippens, et al. (2009). “The emerging roles of serine protease cascades in the epidermis.” Trends Biochem Sci 34(9): 453-463.

Pavlopoulou, A., G. Pampalakis, et al. (2010). “Evolutionary history of tissue kallikreins.” PLoS One 5(11): e13781.

Ramakrishna, S., S. W. Cho, et al. (2014). “Surrogate reporter-based enrichment of cells containing RNA-guided Cas9 nuclease-induced mutations.” Nat Commun 5: 3378.

Smith, C. E., A. S. Richardson, et al. (2011). “Effect of kallikrein 4 loss on enamel mineralization: comparison with mice lacking matrix metalloproteinase 20.” J Biol Chem 286(20): 18149-18160.

Smith, D. L., J. G. Smith, et al. (1995). “Netherton’s syndrome: a syndrome of elevated IgE and characteristic skin and hair findings.” J Allergy Clin Immunol 95(1 Pt 1): 116-123.

Stefansson, K., M. Brattsand, et al. (2006). “Kallikrein-related peptidase 14 may be a major contributor to trypsin-like proteolytic activity in human stratum corneum.” Biol Chem 387(6): 761-768.

Stefansson, K., M. Brattsand, et al. (2008). “Activation of proteinase-activated receptor-2 by human kallikrein-related peptidases.” J Invest Dermatol 128(1): 18-25.

Talieri, M., M. Devetzi, et al. (2012). “Human kallikrein-related peptidase 12 (KLK12) splice variants expression in breast cancer and their clinical impact.” Tumour Biol 33(4): 1075-1084.

Terao, M., M. Tamano, et al. (2016). “Utilization of the CRISPR/Cas9 system for the efficient production of mutant mice using crRNA/tracrRNA with Cas9 nickase and FokI-dCas9.” Exp Anim 65(3): 275-283.

Valton, J., J. P. Cabaniols, et al. (2014). “Efficient strategies for TALEN-mediated genome editing in mammalian cell lines.” Methods 69(2): 151-170.

West, D. B., R. K. Pasumarthi, et al. (2015). “A lacZ reporter gene expression atlas for 313 adult KOMP mutant mouse lines.” Genome Res 25(4): 598-607.

Yen, S. T., M. Zhang, et al. (2014). “Somatic mosaicism and allele complexity induced by CRISPR/Cas9 RNA injections in mouse zygotes.” Dev Biol 393(1): 3-9.

10. Supplement

Supplementary figure 1

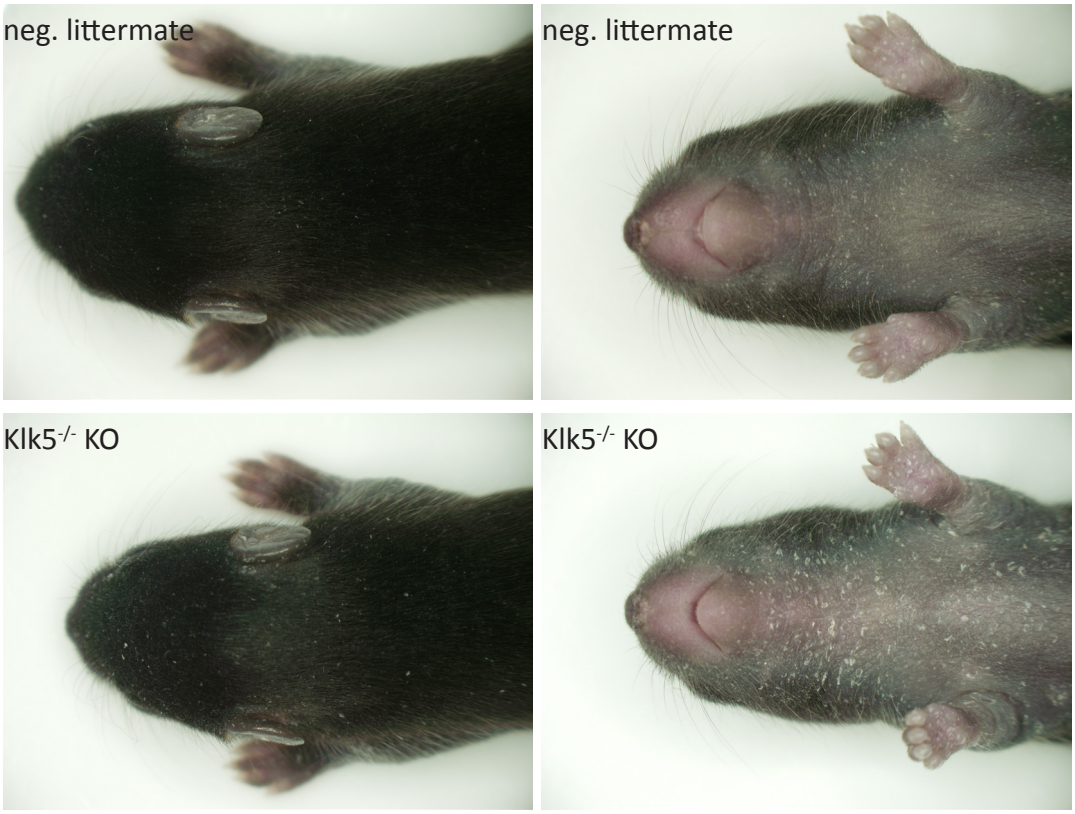

Supplementary figure 1. KLK5 deficient (KO) postnatal day 8 (P8) pups display an increase in epidermal scaling when compared to their wild type (wt) littermates. $Klk5^{tm2a(KOMP)Wtsi}$ ($Klk5^{-/-}$) mice have visible increase of epidermal scaling compared to their negative wild type and heterozygous littermates.

Supplementary figure 2

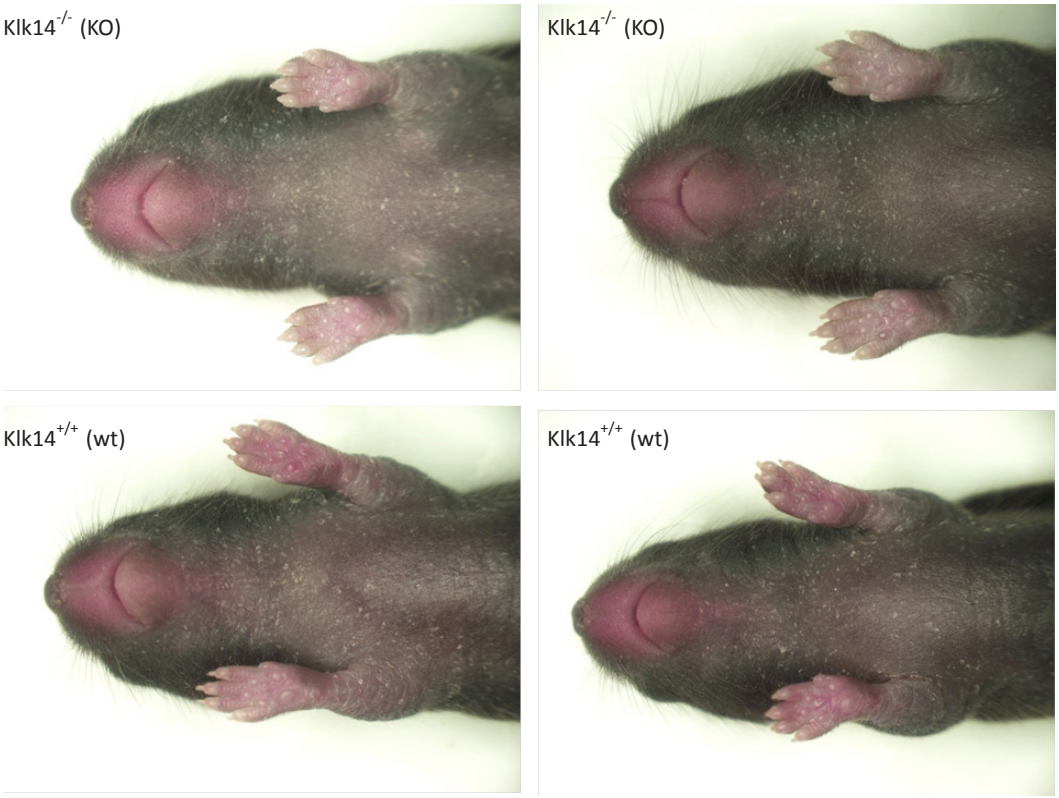

Supplementary figure 2. KLK14 deficient (KO) postnatal day 8 (P8) pups do not differ from their wild type (wt) littermates in respect to epidermal scaling. $Klk14^{tm1b(KOMP)Wtsi}$ ($Klk14^{-/-}$) mice lacking exon 2 of Klk14 (RYDER *et al.*, 2013, WEST *et al.* 2015) do not display an increase in epidermal scaling compared to their wt ($Klk14^{+/+}$) littermates that was observed in both KLK5-deficient and KLK5 and KLK14 double-deficient knock-out animals at P8.

Supplementary figure 3

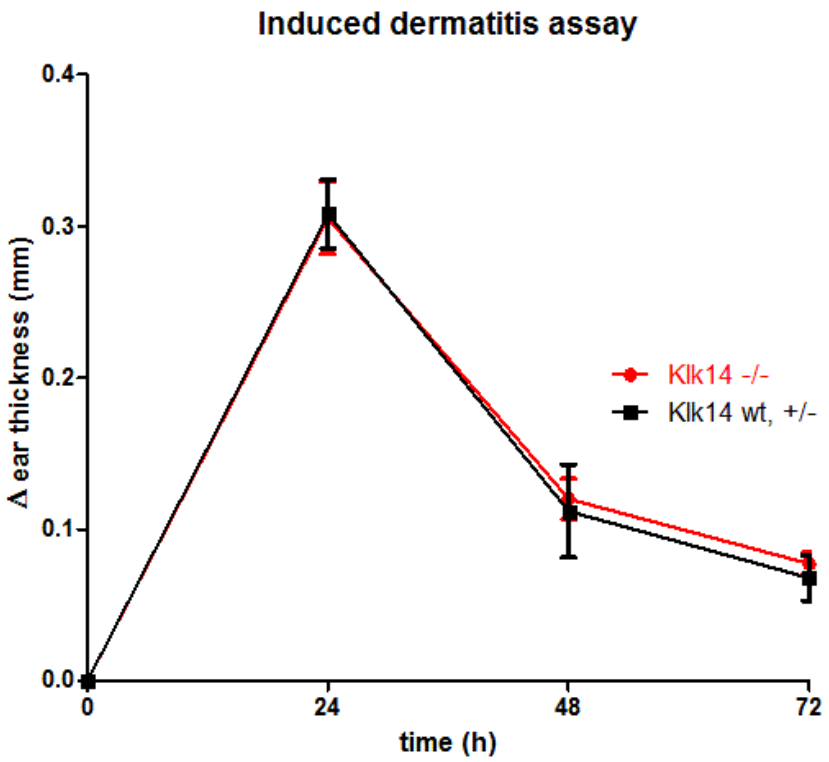

Supplementary figure 3. Induced dermatitis assay in KLK14-deficient mice. Male Klk14$^{tm1b(KOMP)Wtsi}$ mice from four litters (n=16) aged 8-12 weeks were analyzed. To induce irritation, 30 ul of 2,1 % croton oil was applied on left ear, while 30 ul of vehicle was applied on right ear as control. Ear thickness was measured with a precision caliper at 0, 24, 48 and 72 hours. The average difference between left and right ear thickness in Klk14$^{tm1b(KOMP)Wtsi}$ (Klk14$^{-/-}$) animals was compared to the average difference between left and right ear thickness in heterozygous Klk14$^{-/+}$ and wild type (wt) Klk14$^{+/+}$ for each time point. No difference between the two groups was observed.